METHODS OF TARGETS' CHARACTERIZATION

CH. STODEL, *GANIL*

1. Requirements
2. Characterization's techniques for Actinide Targets
3. Monitoring of targets during irradiation
4. (Post-irradiation characterization)
5. Conclusion

Talk of A. Mitu

I-REQUIREMENTS

1. Neutron-induced reaction
2. Heavy Ion induced reaction

REQUIREMENTS – NEUTRON-INDUCED CROSS-SECTION MEASUREMENTS

P. Schillebeeckx et al., NIMA 613 (2010) 378-385

- Fuel cycle, criticality safety studies of spent fuel storages and transportation: total and capture cross-sections requested with an uncertainty less 2%
- Thorium-Uranium fuel cycle: neutron-induced capture cross-section of ^{232}Th with an uncertainty better than 2%
- Astrophysics: Cross-section of key isotopes for s-process determined with uncertainties of about 1%
- Standards database requested by the IAEA: cross-section data with uncertainties below 1%

NEUTRON-INDUCED CROSS-SECTION MEASUREMENTS

P. D'Hondt et al, Ann. Nucl. Energy vol 11 N°10 pp 485-488, 1984 "Measurement of the thermal-neutron induced fission cross-section of ^{238}U"

2 ^{238}U samples with 170 or 12 ppm ^{235}U

$$\sigma_f^{meas} = \sigma_f^{238U} + \alpha(\%) * \sigma_f^{235U} + \beta(\%) * \sigma_f^{239Pu}$$

587,6 (±2,6) µbarns

741,9 barns

$$^{238}U(n,\gamma)^{239}U \xrightarrow[t_{1/2} = 23.5\,min]{\beta^-} {}^{239}Np \xrightarrow[t_{1/2} = 2.355\,day]{\beta^-} {}^{239}Pu.$$

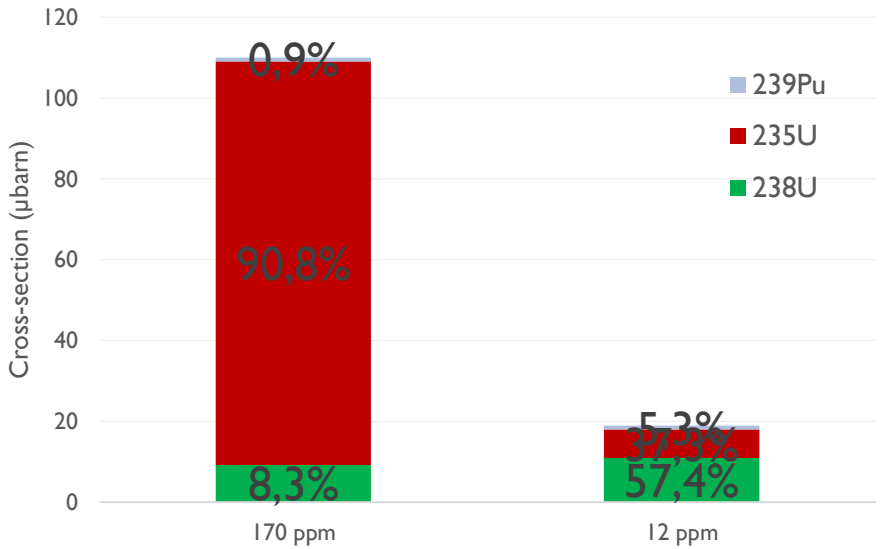

REQUIREMENTS – FUSION-EVAPORATION REACTIONS

Thickness & homogeneity → ions Kinematics

→ Optimal tuning of the spectrometer :

transmission of desired residues

and control of unwanted particles

→ Accuracy (< 5%)

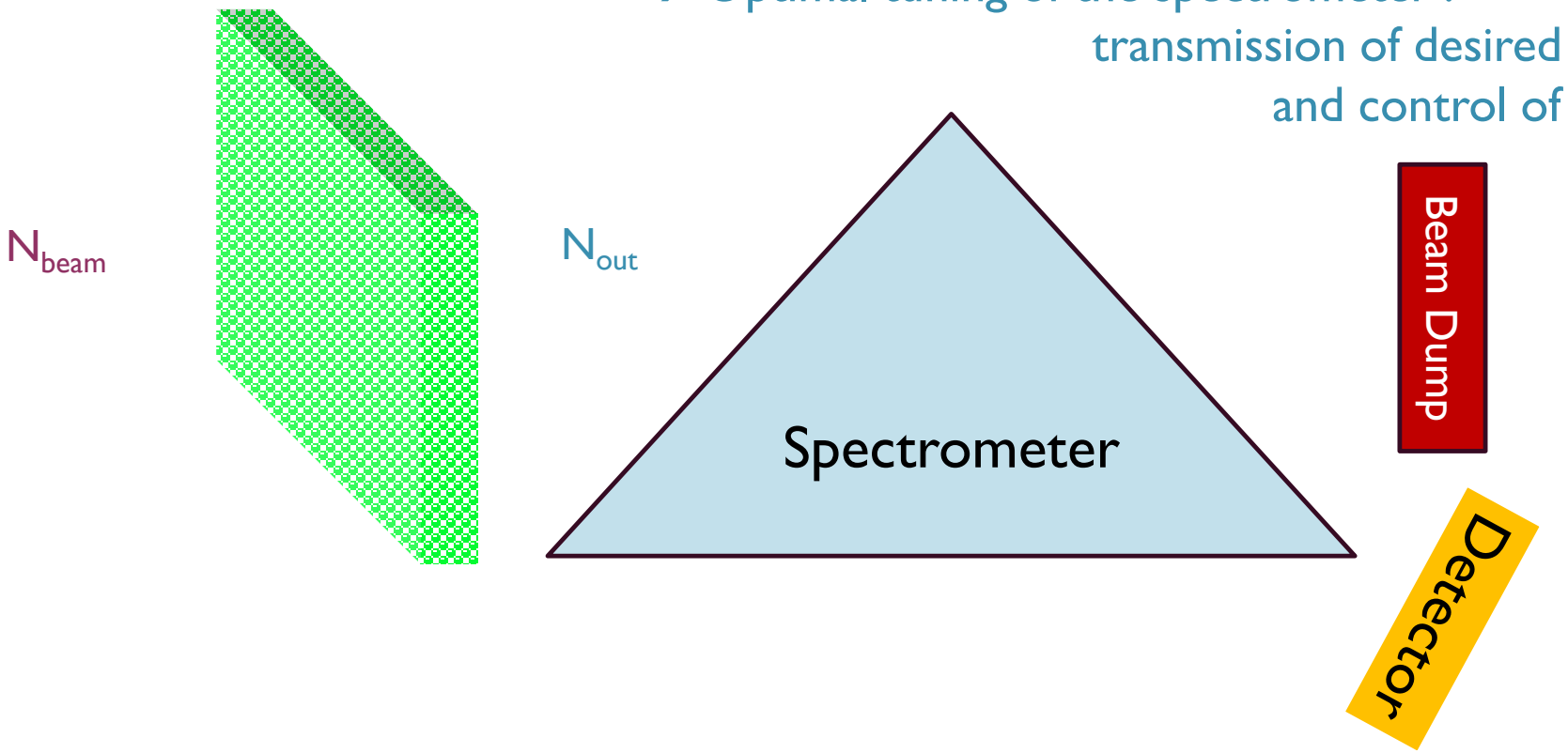

REQUIREMENTS

$$\sigma\ (cm^2) = \frac{N_{out}}{N_{beam} * n_{target}(\frac{at}{cm^2})}$$

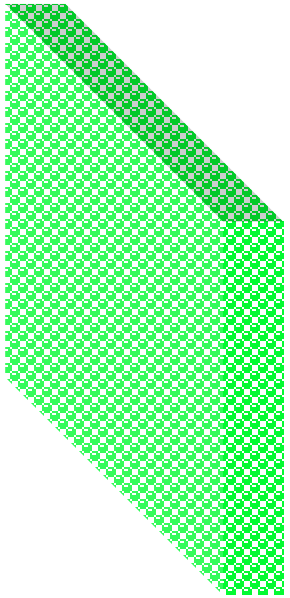

Successful experiment
= Accurate measurements + low background + safe conditions
→ Need of high quality targets with known properties at any time

- Areal density
- Homogeneity == spatial distribution (to be verified experimentally), ensure that all detected neutrons have traversed the same path lenght in the target (no hole) for a correct interpretation of capture and transmission cross-section in resonance regions.
- Quantification & identification of contaminants and impurities, uncertainty depends on their impact on the measurement.
- Effective area

D. Sapundjiev et al., Nucl. Instr. Meth. A 686 (2012) 75-81 "Preparation and characterization of thin film nuclear targets for neutron physical measurements"

CHARACTERIZATION OF ACTINIDE TARGETS

Techniques

1. Low geometry α-particle (LGA)
2. Radiographic Imaging (RI)
3. Thermal Ionization Mass Spectroscopy (TIMS)
4. Neutron Activation Analysis (NAA)
5. PhotoElectron Spectroscopy (XPS)
6. Energy Dispersive X-Ray Spectroscopy (EDS)
7. Particle Induced X-ray Emission (PIXE)
8. Rutherford Back Scattering (RBS)

Properties

Thickness & homogeneity

Chemical identification

Isotopic abundances

(AFM - Surface roughness/structure)

Low Geometry α-Particle (LGA method): Activity measurements

IRMM/JRC – Geel

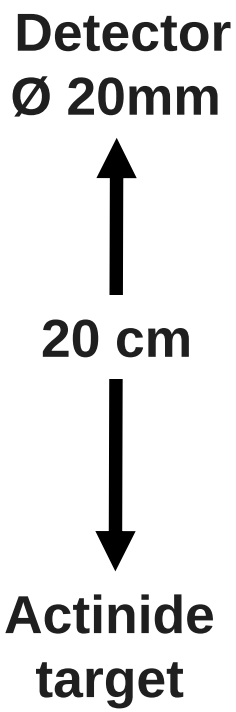

LG3 (variable distance target-detector)

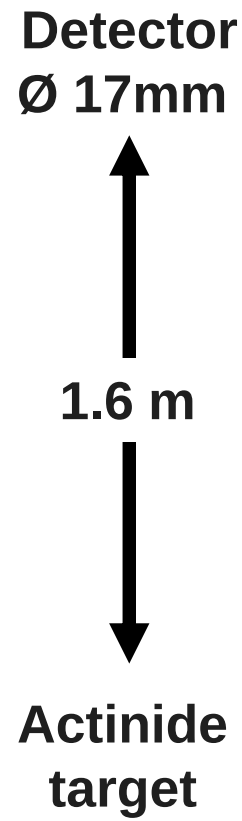

LG2 (fixed distance, high activity)

Low Geometry α-Particle (LGA method): Activity measurements

S. Pomme, Metrologia 52 S73 "The uncertainty of counting at a defined solid angle"

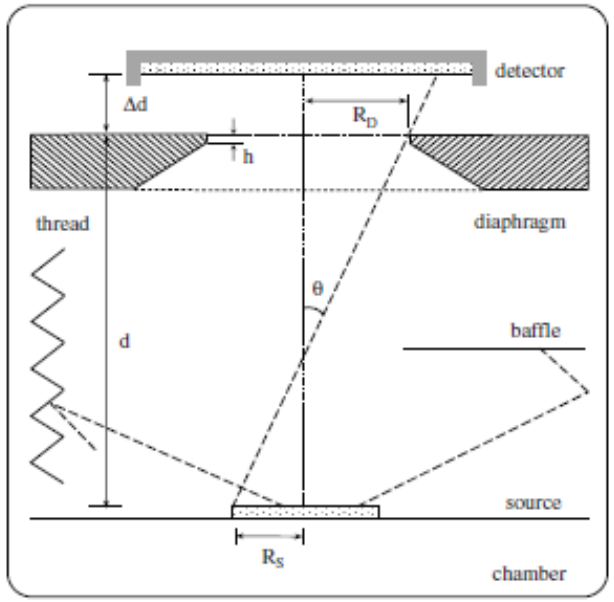

Figure 1. Schematic representation of characteristic geometrical parameters.

Assumptions: isotopic emission of particles, moving undisturbed along a straight line and counted when they hit the detector

Sources of uncertainty:

1. source-detector geometry
2. Solid-angle calculation
3. Energy loss & self absorption
4. Scattering
5. Detection efficiency

$$A = \frac{4\pi \cdot R}{\Omega \cdot \varepsilon}$$

Uncertainties ~ 0,02% *feasible*

Homogeneity

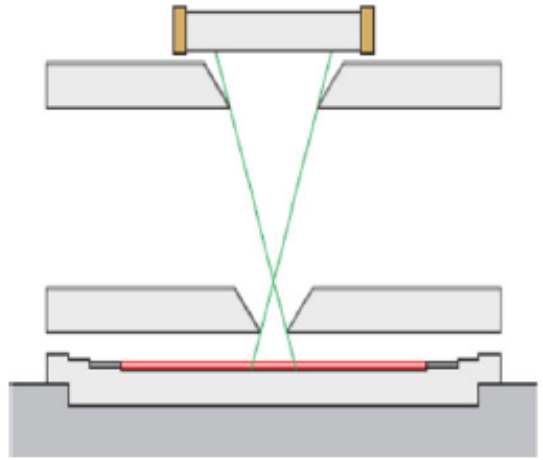

Fig. 3 Schematic representation of the homogeneity measurements geometry. An extra diaphragm is placed above the sample scanning the spatial resolution of the radioactive source

See also D.M. Gilliam et al, J. Radioanal. Nucl. Chem. 299 (2014) 1061-1065 "Improvements in the characterization of actinide targets by low solid-angle counting"

Low Geometry α-Particle (LGA method): Activity measurements

G. Sibbens et al, J. Radioanal. Nucl. Chem. 299 (2014) 1093-1089 "Preparation of ^{240}Pu and ^{242}Pu targets to improve cross-section measurements for advanced reactors and fuel cycles" (15 – 240 µg/cm²)

Dead time < 5µs
Background count rate < 0,003 pps
ε = 100%
Ω = 0,0007 % 4 π sr
20 spectra of 500 s or 7000 s

$$\frac{u(M)}{M}\left(^{240,242}Pu\right) = 0{,}5\text{-}0{,}9\ \%$$

$$A = \frac{4\pi \cdot R}{\Omega \cdot \varepsilon}$$

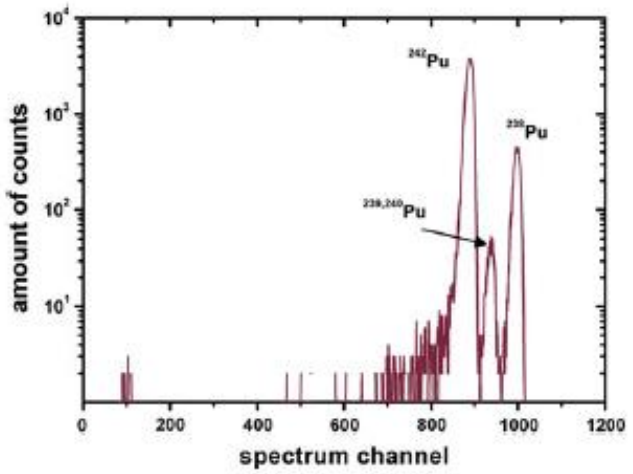

Fig. 3 Alpha-particle spectrum of a ^{242}Pu target measured with the IRMM LG3 counter

$$M_\alpha = \frac{4\pi}{\Omega \cdot \varepsilon} \cdot \frac{C_\alpha}{B}$$

B: Intrinsic specific activity of the sample deduced using « Thermal Ionization Mass Spectrometry » TIMS (next slide)

J. Heyse et al., J. Radioanal. Nucl. Chem. (2014)299:1055-1059 "Characterization of ^{235}U for the development of a secondary neutron fluence standard"

$$\frac{u(M)}{M} = 0{,}3 - 0{,}4\%$$

$$\frac{\delta M}{M}(\pm 35mm) = 5\ \%$$

RADIOGRAPHIC IMAGING : HOMOGENEITY & THICKNESS OF THE TARGET LAYER DEPOSIT

D. Liebe et al, Nucl. Instr. Meth. A590 (2008) 145-150 "The application of neutron activation analysis, scanning electron microscope, and radiographic imaging for the characterization of electrochemically deposited layers of lanthanide and actinide elements"

1 Production of ^{244}Pu target

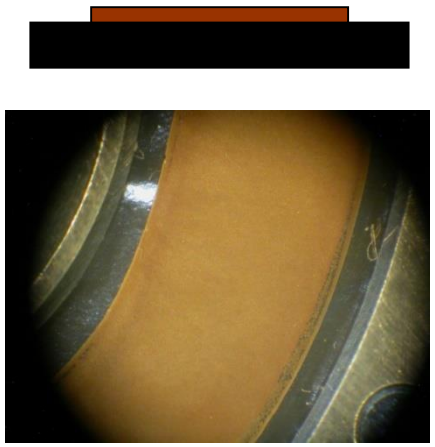

Crystallites, sizes of 25 or 50 µm (depending on the IP), into a stable exited state by radiation.

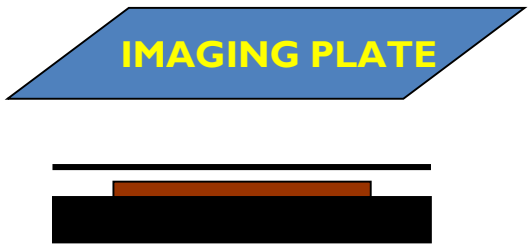

2 Imaging plate exposure to active target (≈ 6h)

Radioactive targets or targets with active tracers

3 Imaging plate reading process

luminescence light → arbitrary unit
Photo Simulated Luminescence (PSL) α radiation

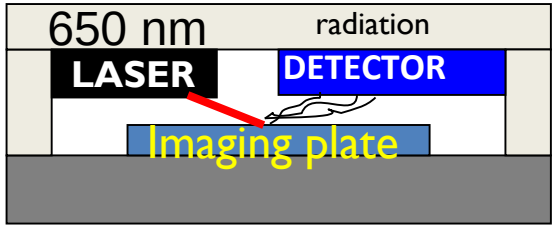

Courtesy of K. Eberhardt

RADIOGRAPHIC IMAGING : HOMOGENEITY & THICKNESS OF THE TARGET LAYER DEPOSIT

Targets for ^{242}Pu(n,f)-measurements at n-ELBE (FZDR). Backing: Si-wafer, sputtered with thin Ti-layer. In total: 37 mg ^{242}Pu for 8 targets

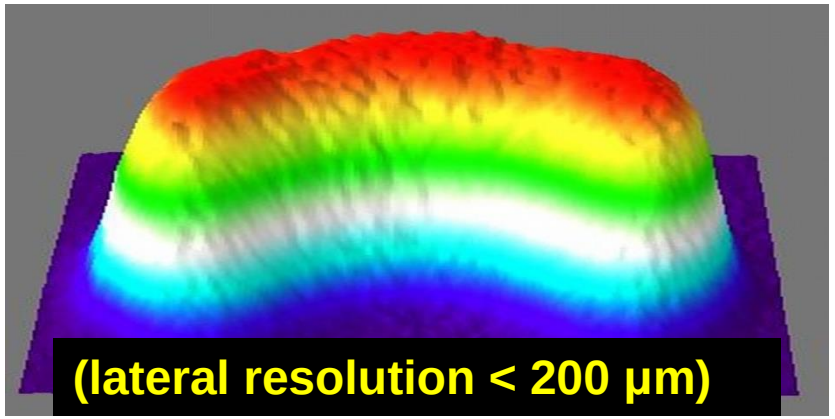

D. Liebe et al, Nucl. Instr. Meth. A590 (2008) 145-150 "The application of neutron activation analysis, scanning electron microscope, and radiographic imaging for the characterization of electrochemically deposited layers of lanthanide and actinide elements"

^{238}U deposit – resolution of 42 µm

G. Sibbens et al, AIP Conf. Proc. 1962, 030007-1-9

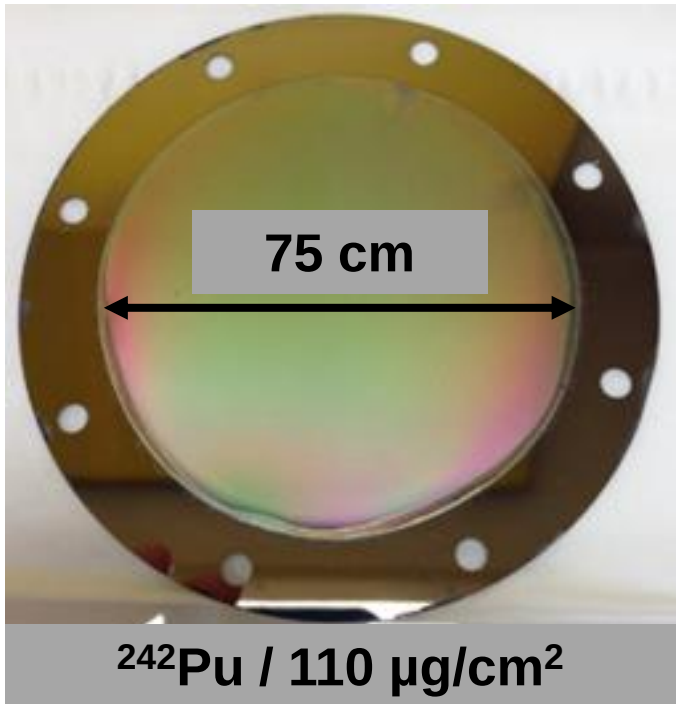

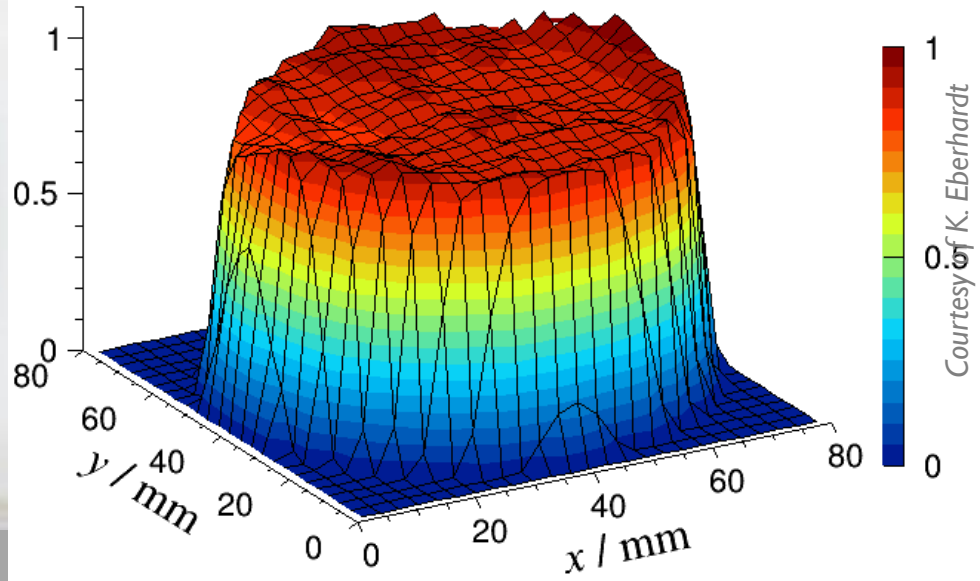

RADIOGRAPHIC IMAGING : HOMOGENEITY & THICKNESS OF THE TARGET LAYER DEPOSIT

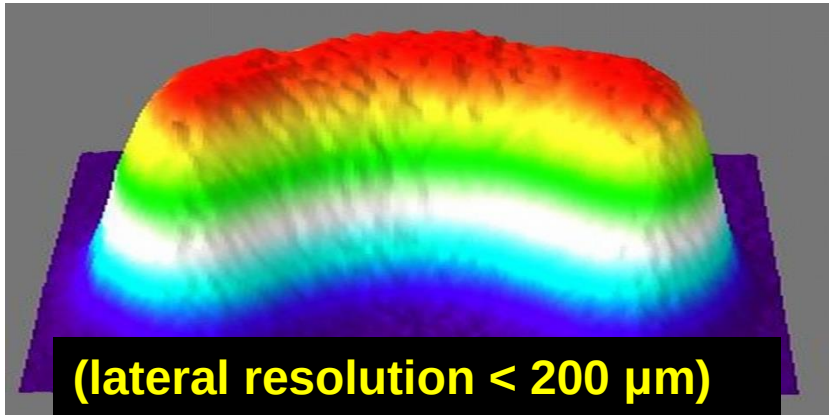

D. Liebe et al, Nucl. Instr. Meth. A590 (2008) 145-150 "The application of neutron activation analysis, scanning electron microscope, and radiographic imaging for the characterization of electrochemically deposited layers of lanthanide and actinide elements"

Comparisons to the measured values of a microbalance with a reference sample

Table 1
Thicknesses of the UF_4-targets by microbalance at GSI and the FLA 7000 system

Target no.	Thickness determined by FLA 7000 (µg/cm^2) S.D. ±5.2%[a]	Thickness determined by microbalance[b] (µg/cm^2)	Deviation (%)
1	"Standard"	389	0.0
2	376	377	0.2
3	360	364	1.0
4	363	369	1.5
5	363	381	4.6
6	365	372	1.9

[a]Standard deviation for 6h exposure, sensitivity 10^4, pixel size 25µm, dynamic range 10^5, pixel depth 16bit.
[b]Mettler Toledo XP 205, measuring accuracy: 0.01 mg in the range from 0 to 50 mg.

Courtesy of K. Eberhardt

THERMAL IONIZATION MASS SPECTROMETRY (TIMS) : ISOTOPIC ABUNDANCES

S. Richter et al, Int. J. of Mass Spectrometry 229 (2003) 181-197 "Improved techniques of high accuracy isotope ratio measurements of nuclear materials using thermal ionization mass spectrometry"

Eluted fraction of active solution evaporated, dissolved and deposited on a filament

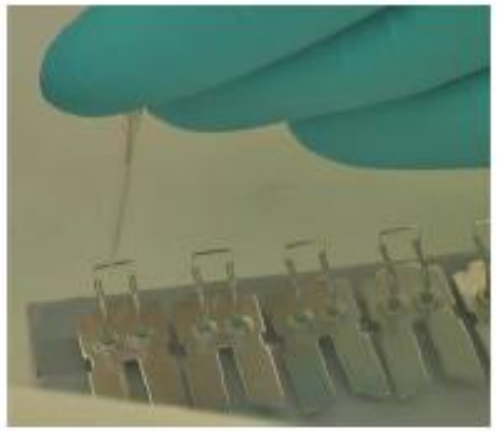

Fig. 2 Deposition of a drop of 1 µL solution containing about 50 ng Pu on the thenium filament

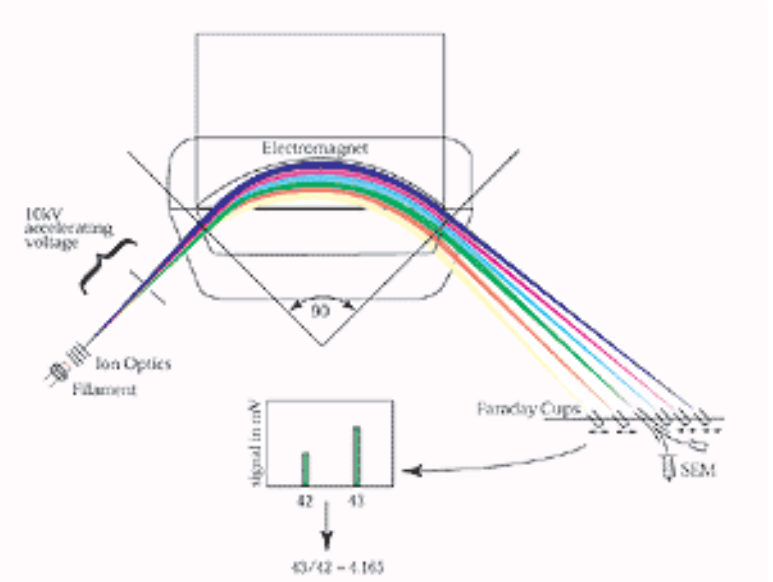

G. Sibbens et al, J. Radioanal. Nucl. Chem. 299 (2014) 1093-10989

NEUTRON ACTIVATION ANALYSIS : DEPOSITION YIELD & AVERAGE THICKNESS OF THE DEPOSITED MATERIAL

P. Robouch et al, Nucl. Instr. Meth. A 480 (2002) 128-132 "Target preparation and neutron activation analysis: a successful story at IRMM"

Gamma spectrometry measurements of samples irradiated with neutrons in a nuclear reactor:

$$ {}^{N}_{Z}A(n,\gamma)\ {}^{N+1}_{Z}A $$

Comparison of unknown sample (A_x) and a known standard (A_{st})

elemental m: $m_x = m_{st}(A_x/A_{st})$

D. Liebe et al, Nucl. Instr. Meth. A590 (2008) 145-150 "The application of neutron activation analysis, scanning electron microscope, and radiographic imaging for the characterization of electrochemically deposited layers of

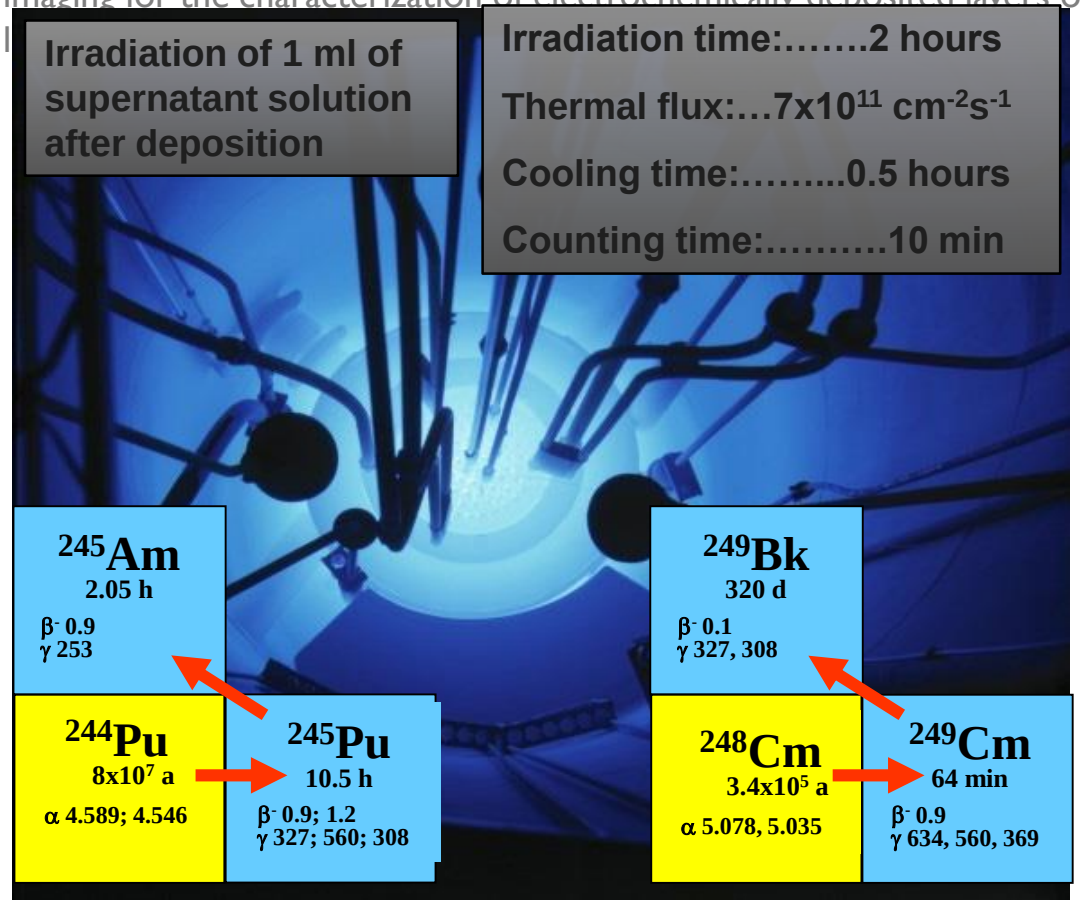

NEUTRON ACTIVATION ANALYSIS : DEPOSITION YIELD & AVERAGE THICKNESS OF THE DEPOSITED MATERIAL

D. Liebe et al, Nucl. Instr. Meth. A590 (2008) 145-150 "The application of neutron activation analysis, scanning electron microscope, and radiographic imaging for the characterization of electrochemically deposited layers of lanthanide and actinide elements"

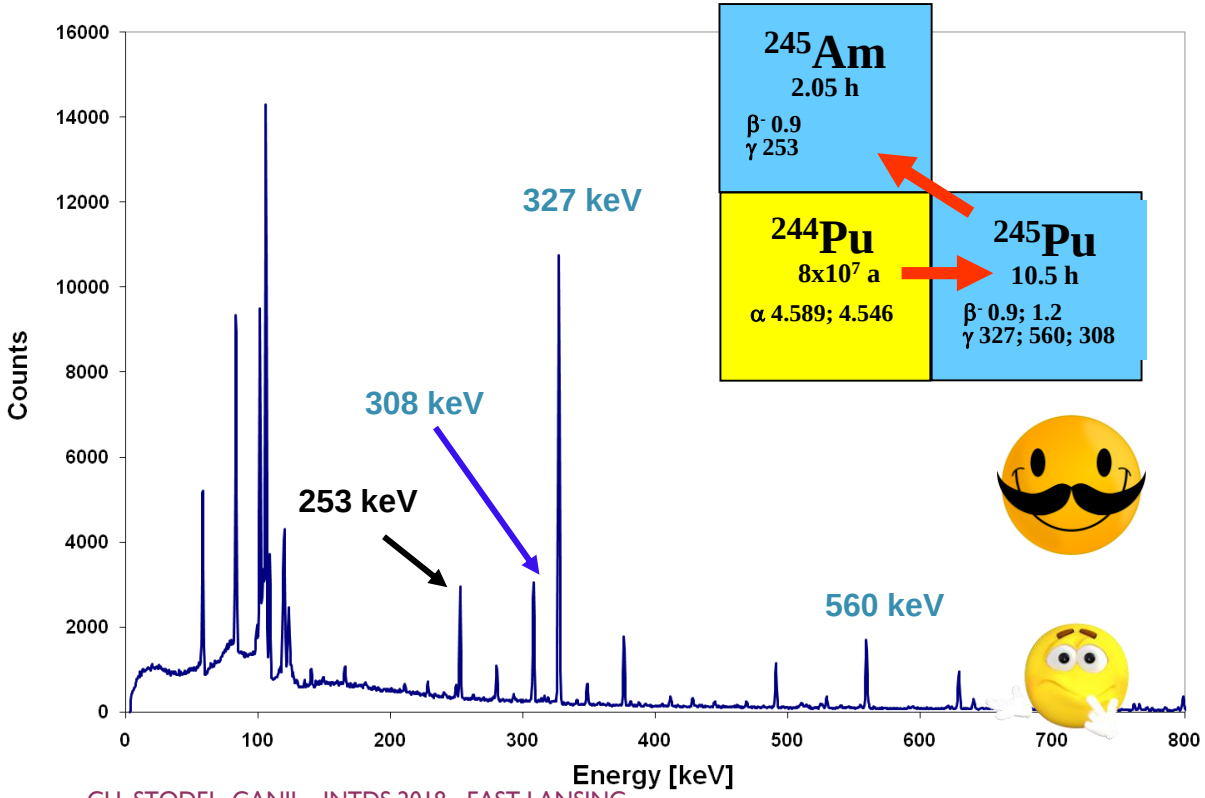

Simultaneous determination of up to 30-40 elements with low detection limit (lanthanide and actinide 0,1-10 ppb)

Time consuming (irradiation + cooling time)

Neutron source

X-RAY PHOTO ELECTRON SPECTROSCOPY (XPS): IMPURITIES

Peak shape and intensity of the photoelectron peaks determines :

- Elemental identity
- Chemical state
- Quantity

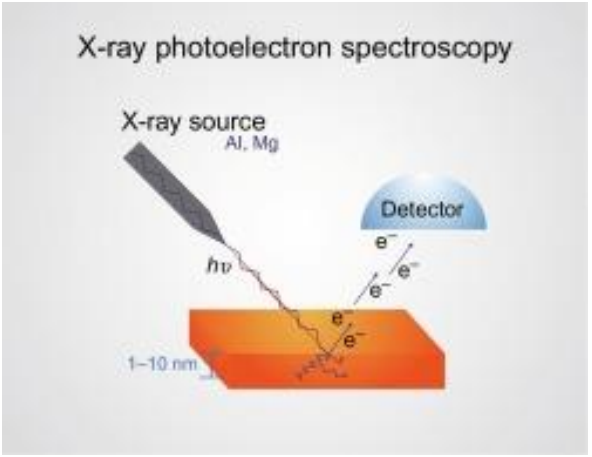

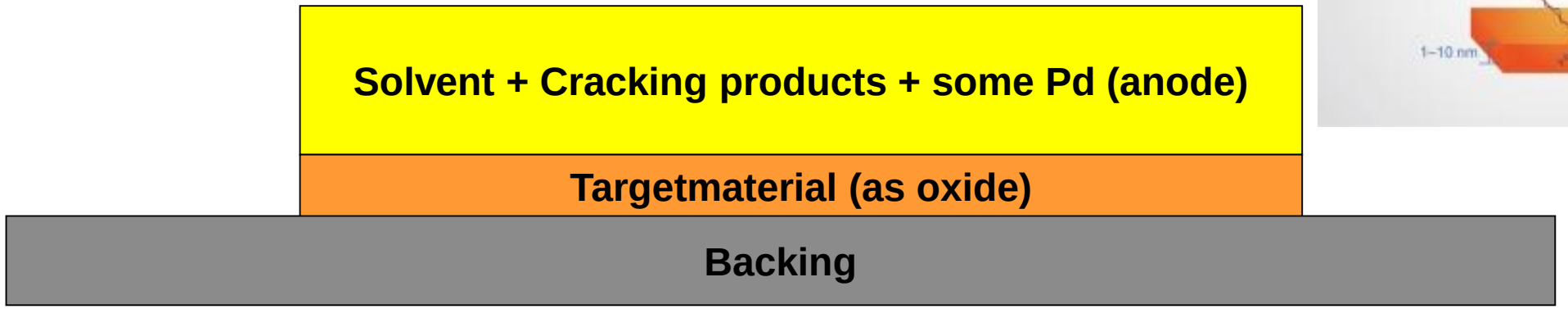

XPS analysis before and after sputtering with ions (Ar^+)

Photoelectronspectroscopy (XPS) of targets produced by MP

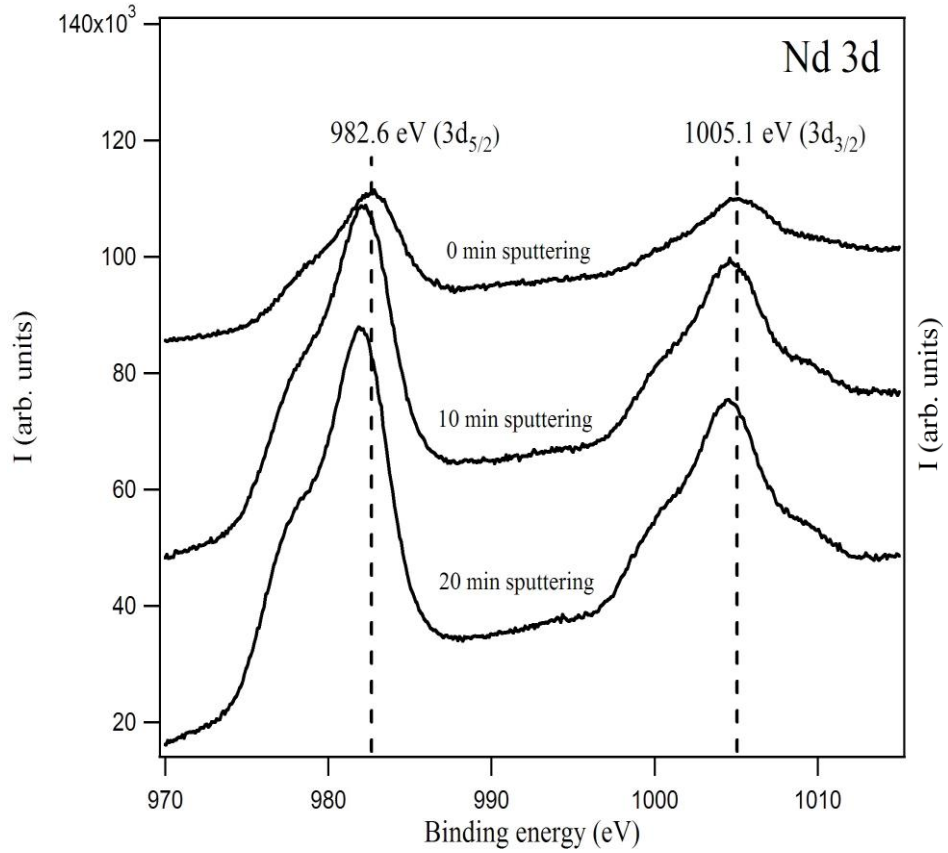

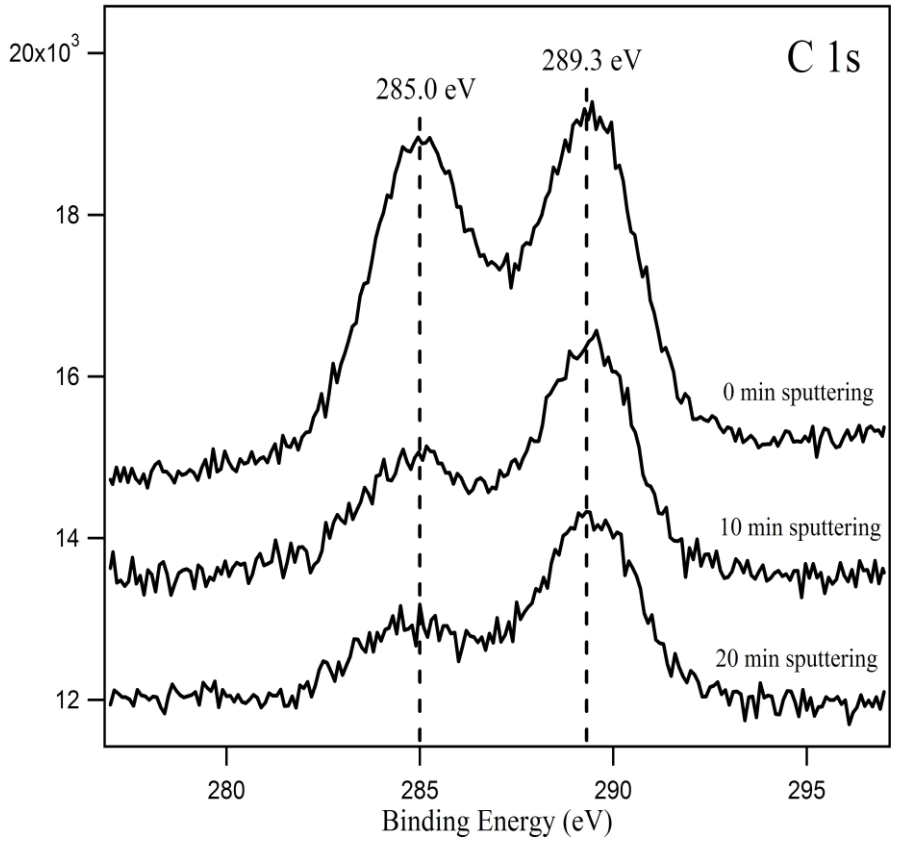

- **Nd 3d signal: grows after Ar^+ sputtering**
- **C 1s signal:**
  285.0 eV is aliphatic carbon → removed after sputtering: physisorbed
  289.3 eV is C(O)OR or COOM group → not removed after sputtering: chemisorbed

A.Vascon et al, Nucl. Instr. Meth.A 714 (2013) 163-175 "Smooth crack-free targets for nuclear applications produced by molecular plating"

ENERGY DISPERSIVE X-RAY SPECTROMETRY (EDS): CHEMICAL COMPOSITION

D. Liebe et al, Nucl. Instr. Meth. A590 (2008) 145-150 "The application of neutron activation analysis, scanning electron microscope, and radiographic imaging for the characterization of electrochemically deposited layers of lanthanide and actinide elements"

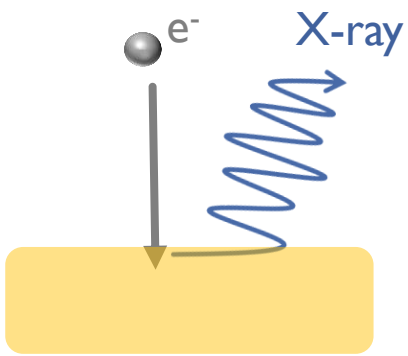

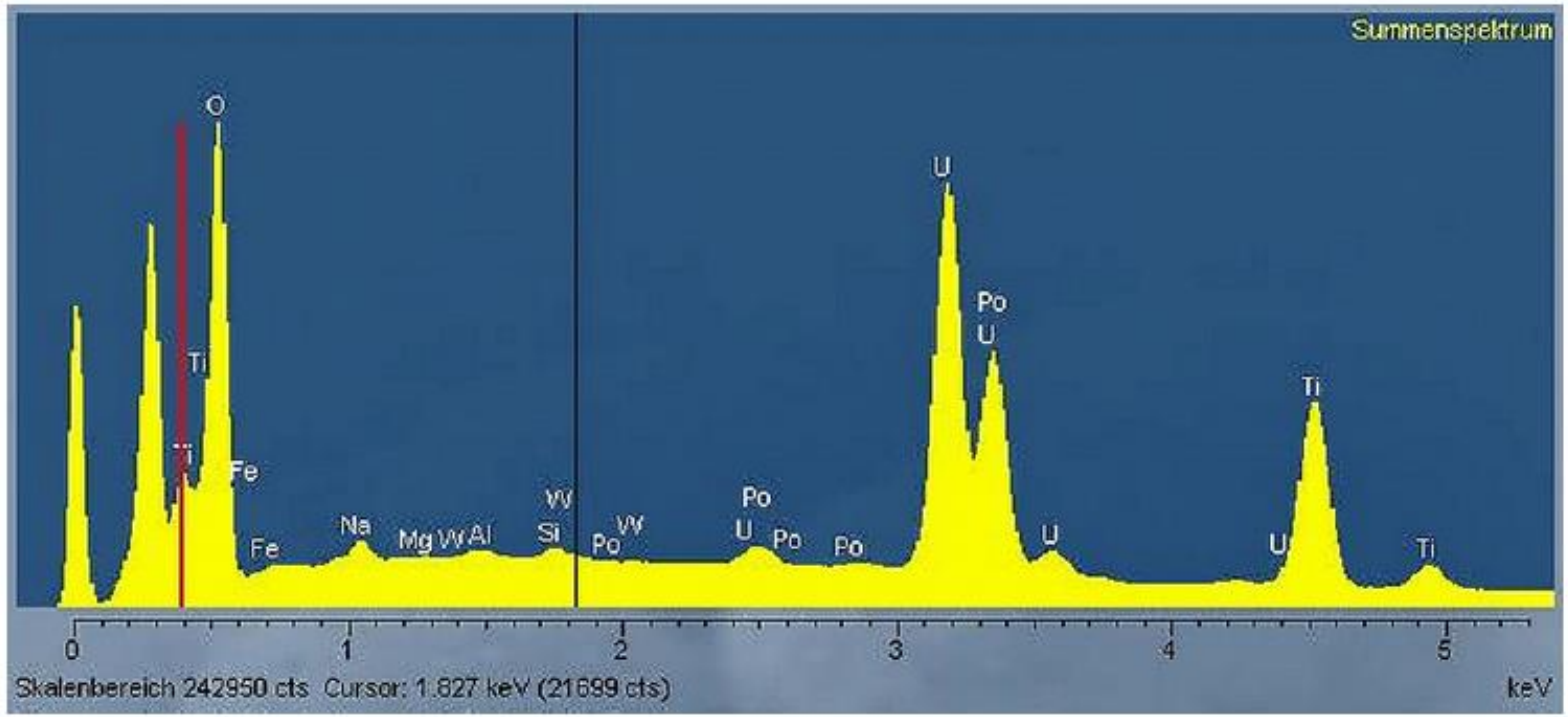

Fig. 3. EDX spectrum of U on a Ti backing.

PARTICLE INDUCED X-RAY EMISSION (PIXE): IMPURITIES

M. Jaskola et al, Nucl. Instr. Meth. A590 (2008) 176-180 "Estimation of the impurity levels in polyimide foils and the life-time of the foils irradiated by charged particle" *(proton 1,5MeV 10-30 nA)*

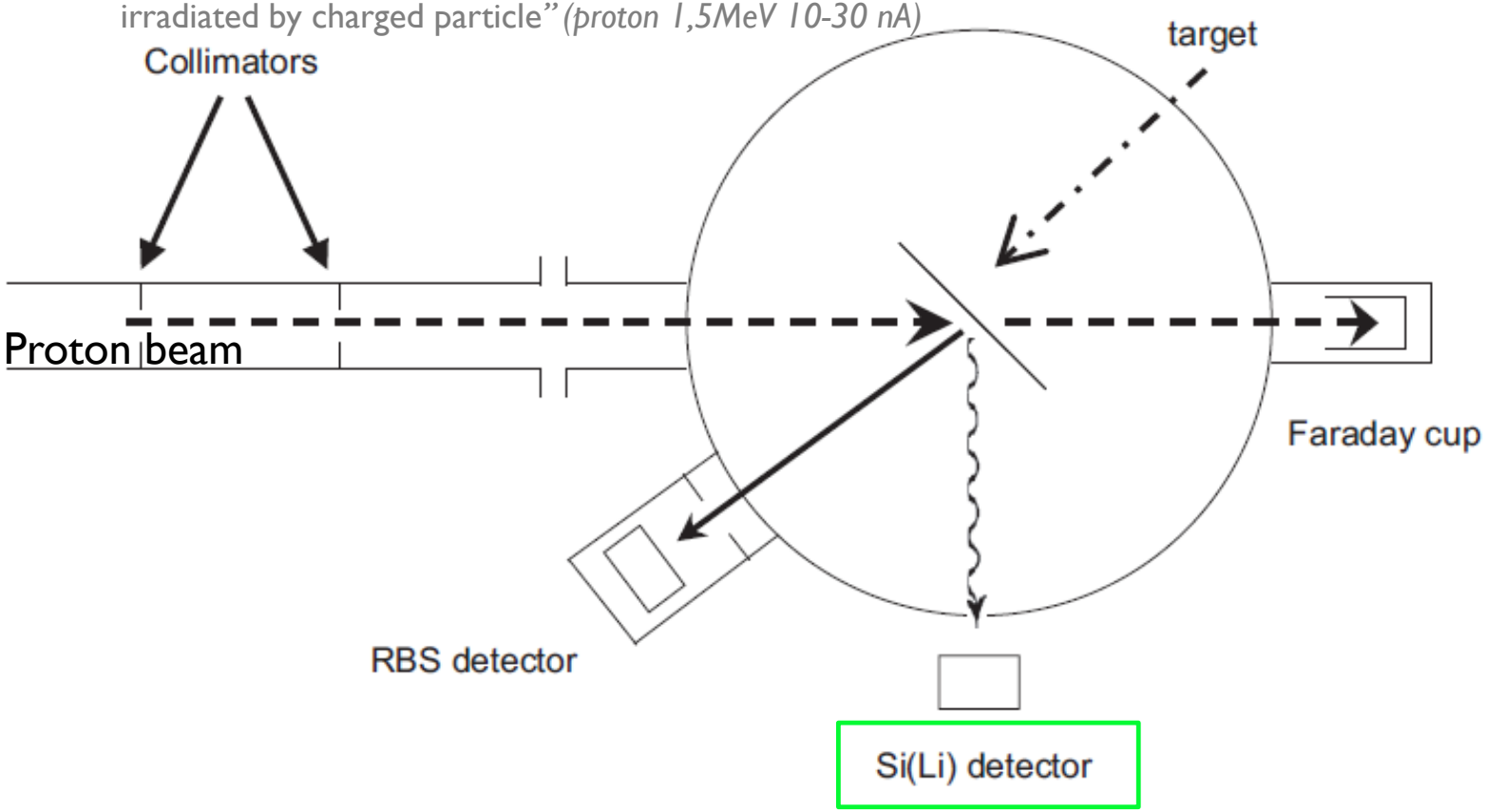

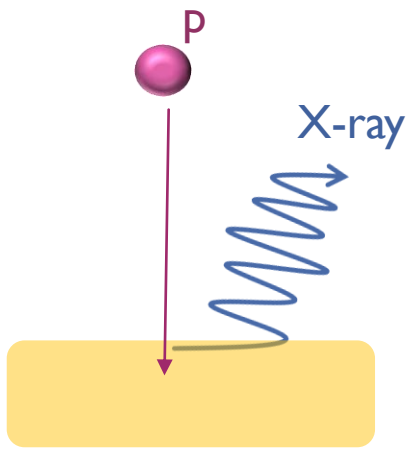

Fig. 1. Experimental set-up for PIXE and RBS measurements.

PIXE TECHNIQUE: IMPURITIES

G. Sibbens et al, Nucl. Instr. Meth. A655 (2011) 47-52 "Quality of polyimide foils for nuclear applications in relation to a new preparation procedure"

Impurities ≈ ng/cm²
For foils of 20-30 µg/cm²

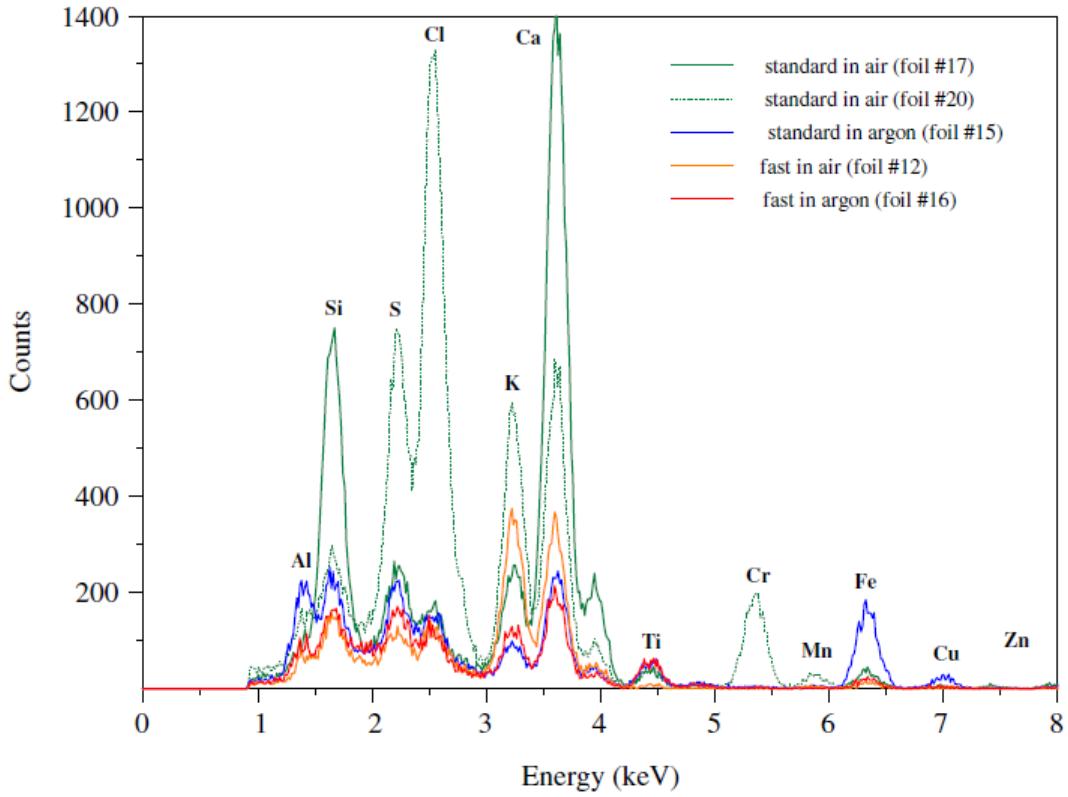

Fig. 5. PIXE energy spectra of the impurities in the samples of the different prepared polyimide foils irradiated by 1.0 MeV protons.

RUTHERFORD BACKSCATTERING (RBS): IMPURITY, CONCENTRATION, THICKNESS

C.O. Bacri et al, J. Radioanal. Nucl. Chem. 299 (2014) 1099-1105 "CACAO facility: radioactive taregts at Orsay" (^{4}He 2,4MeV)

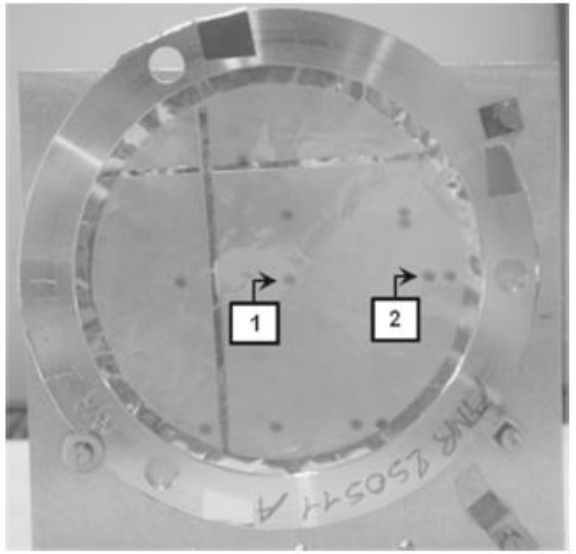

Fig. 1 ^{238}U reference target. The cross is used as a reference for position measurements. *Little spots* are positions where RBS measurements have been done. The points labeled with number *1* and *2* are discussed in the text paragraph "RBS, autoradiography and thickness measurements" and in Fig. 4

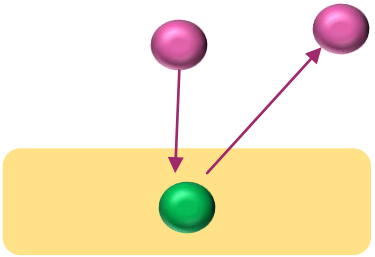

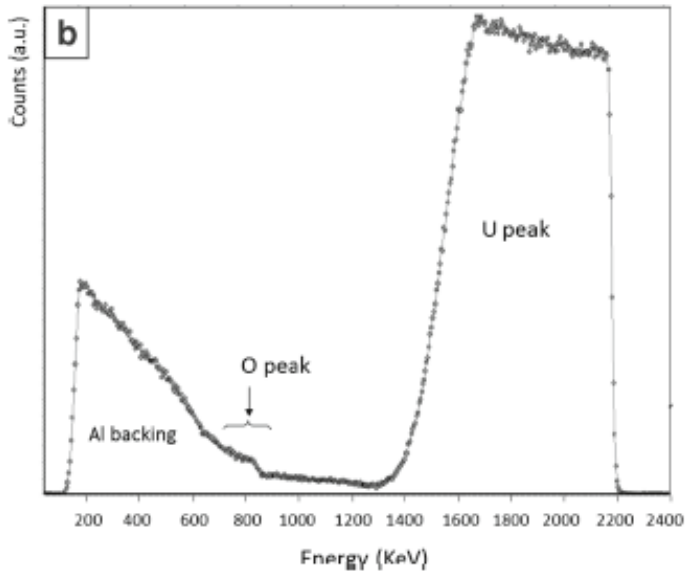

Fig. 3 RBS spectra measured with a 2.4 MeV ^{4}He beam at 165°. **a** Reference Bi target, **b** ^{238}U target

Table 2 U content at two different points on the reference target and obtained by two different techniques: RBS and α-particle counting

Used technique	Point 1	Point 2
RBS	839×10^{15} at/cm^2	$1{,}112 \times 10^{15}$ at/cm^2
α counting	933×10^{15} at/cm^2	$1{,}200 \times 10^{15}$ at/cm^2

Labels of the points refers to those of Fig. 1

MONITORING OF TARGETS

1. Electron attenuation method
2. Tuning on α emission
3. Temperature Monitoring
4. α energy loss
5. Scattered beam/target
6. (Performance/lifetime: C, UCx cases)

ELECTRONS ATTENUATION

Principle : measuring attenuation of electron current using angular scattering and absorption

R. Mann (patent DE 10242962 A1-GSI)

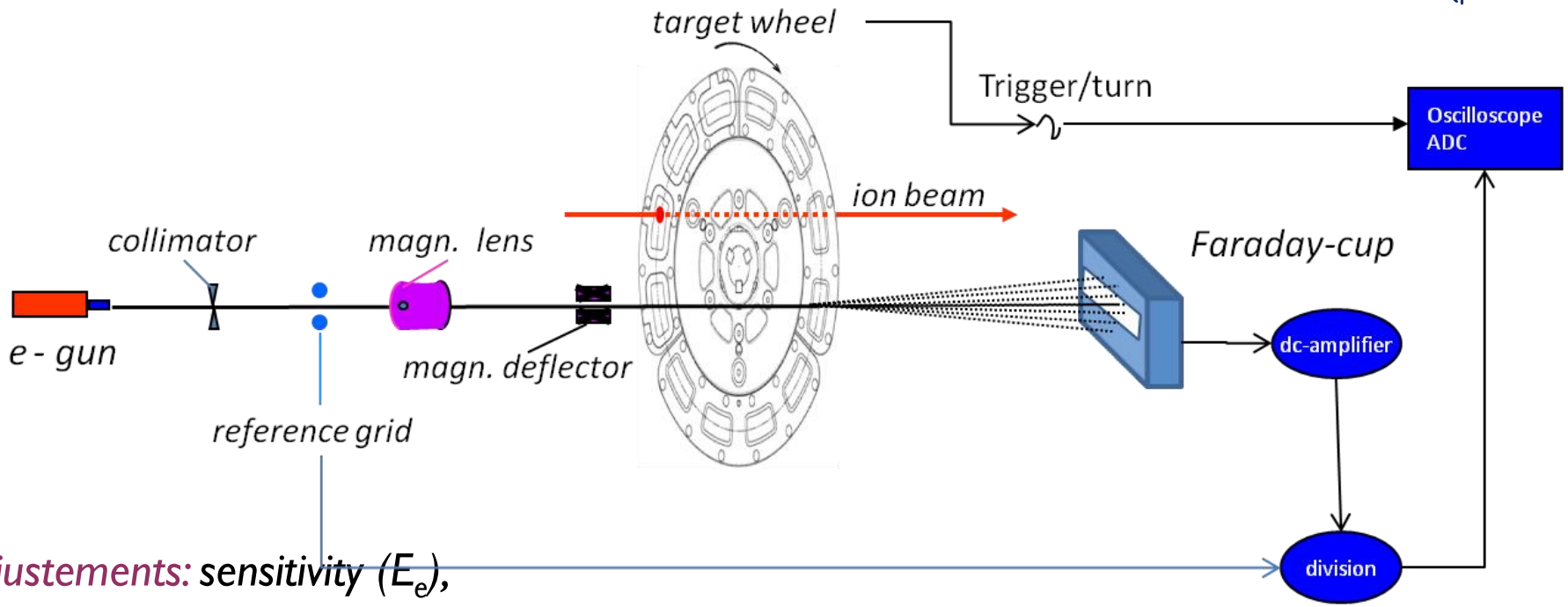

Adjustements: sensitivity (E_e),

resolution ($\leq$ 0.4mm , 15µs)

ELECTRONS ATTENUATION

S. Hofmann et al, Eur. Phys. J.A (2012) 48:12 "The reaction $^{48}Ca + ^{248}Cm \rightarrow ^{296}116^*$ studied at the GSI-SHIP"

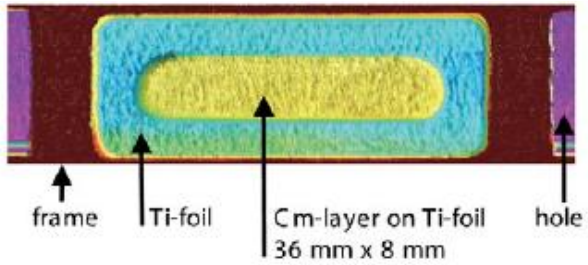

Accuracy ± 2%

On-line Monitoring

R. Mann et al, GSI Report 2004 p.224 "On-line target control"

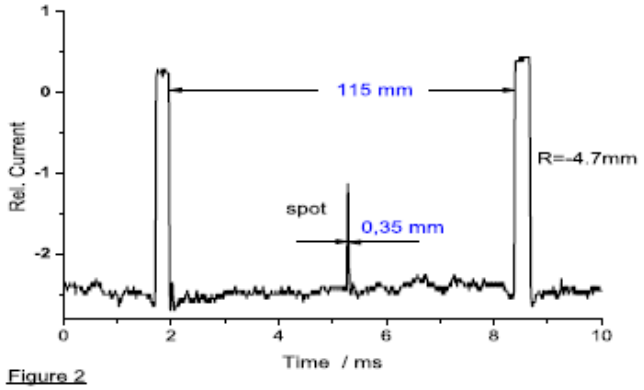

Figure 2

Figure 2 displays the time dependent electron current penetrating one sector of a 440 µg/cm^2 PbS target with a carbon backing of 40 µg/cm^2 and a carbon cover of 10 µg/cm^2. The width of the spokes of the wheel (~4mm) is resolved and a material deposition (spot) is detected with an extension of 0.35 mm in the direction of rotation and at

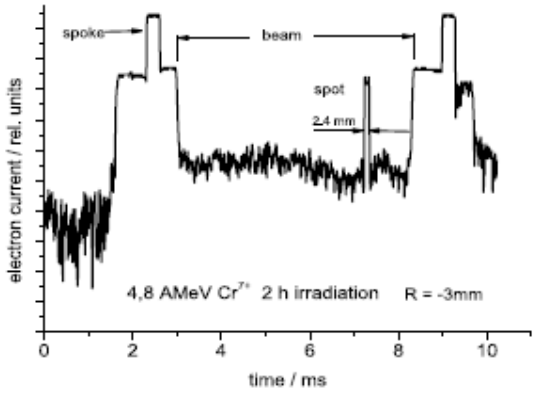

Figure 4

Figure 4 indicates a rapid increase of transparency for the electron beam after only 2 hours irradiation of a BiF_3 target with a ^{54}Cr beam. The BiF_3 compound transformed to a fine granular structure as noticed from scanning electron microscopy.

ELECTRONS ATTENUATION

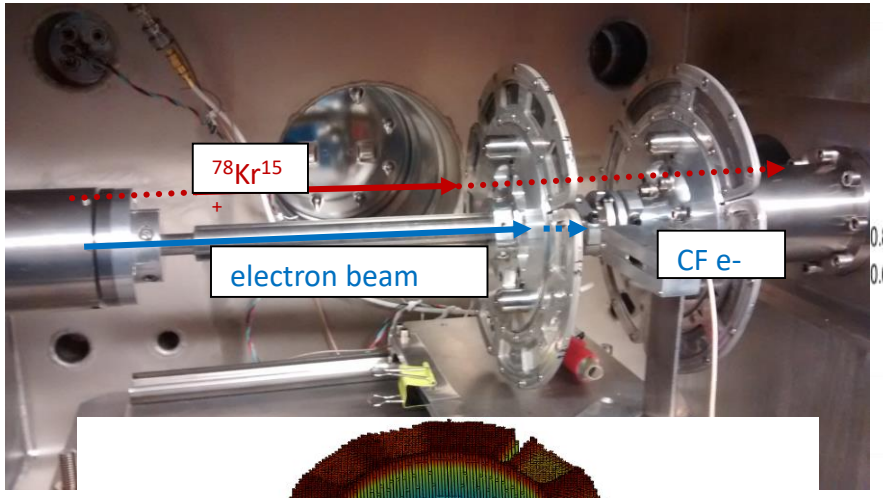

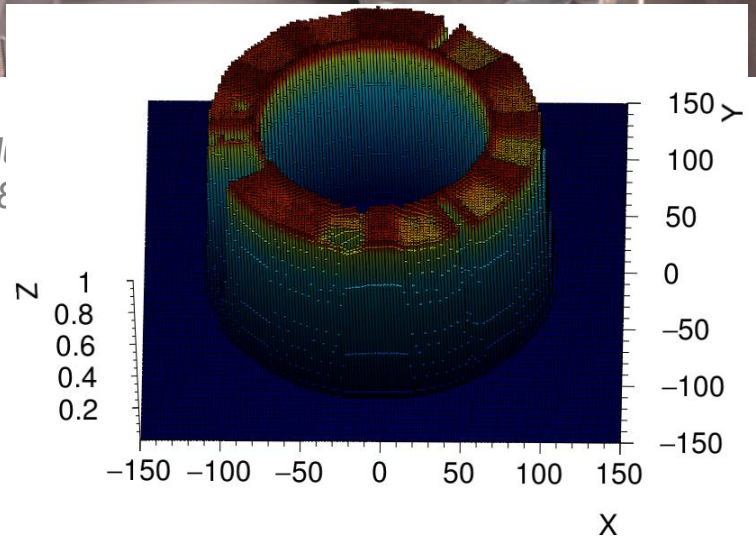

J. Kall
(2008

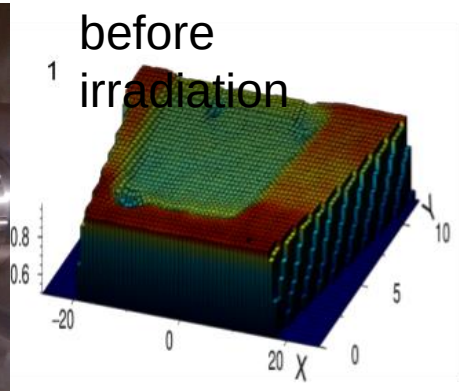

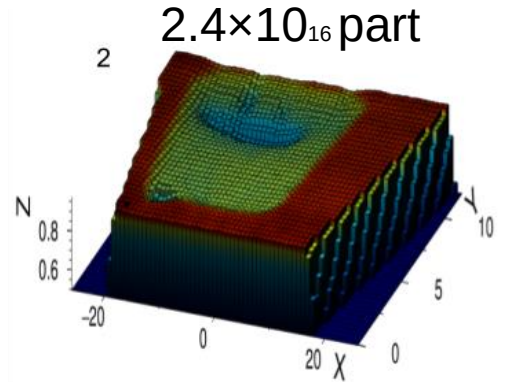

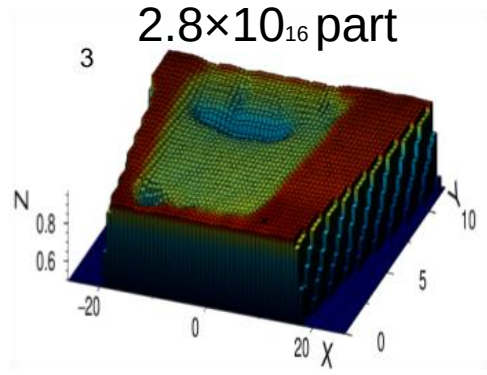

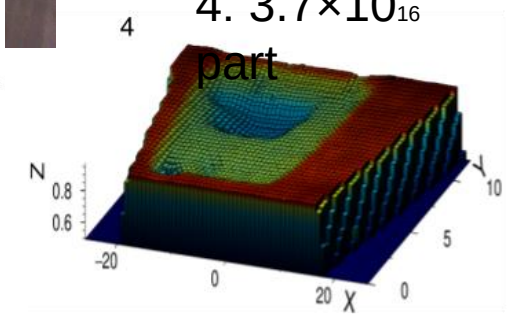

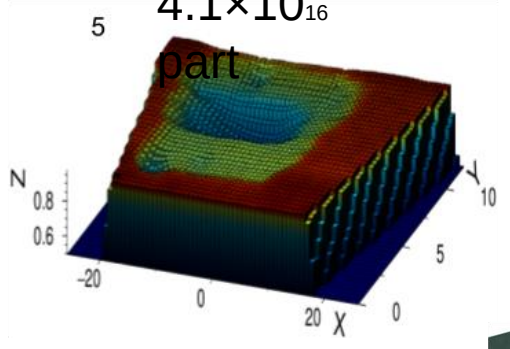

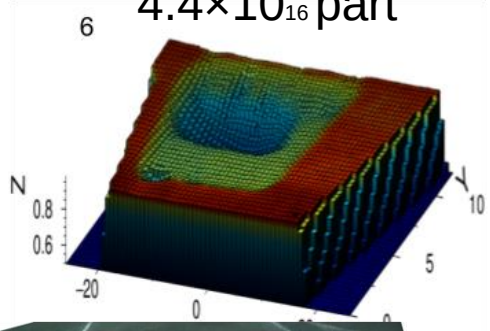

Time evolution of Bi target with beam

Front

⊗

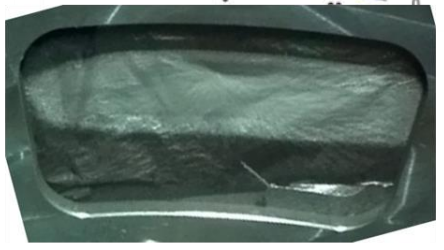

MONITORING OF SHE TARGETS
TUNING ON α EMISSION OF THE TARGETS

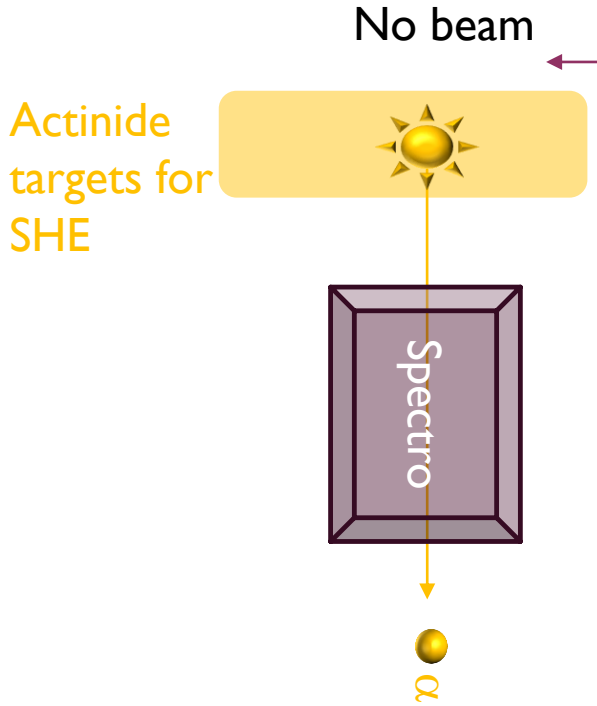

S. Hofmann et al, Eur. Phys. J.A (2012) 48:12 "The reaction ^{48}Ca + $^{248}Cm \rightarrow {}^{296}116^*$ studied at the GSI-SHIP"

^{248}Cm @ 96.85%.

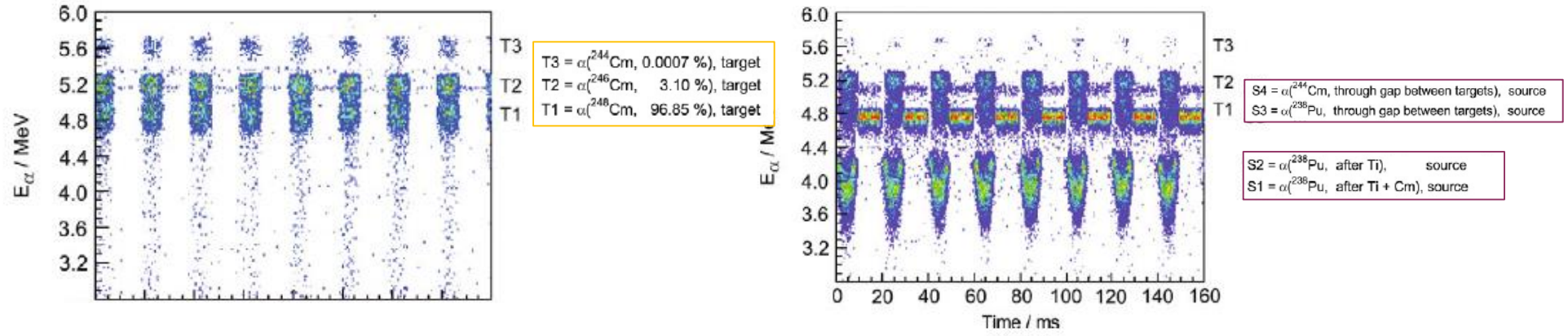

Fig. 2. Energy distribution of α particles emitted from the targets (top) and from the targets plus a ^{238}Pu source moved in front of the targets (bottom). The α energies were measured as function of time for complete turns of the wheel lasting 160 ms. See text for a detailed description.

Time to time checking

MONITORING OF SHE TARGETS TUNING ON α EMISSION OF THE TARGETS

S. Hofmann et al, Eur. Phys. J.A (2012) 48:12 "The reaction $^{48}Ca + ^{248}Cm \rightarrow ^{296}116^*$ studied at the GSI-SHIP"

Conditionning phase

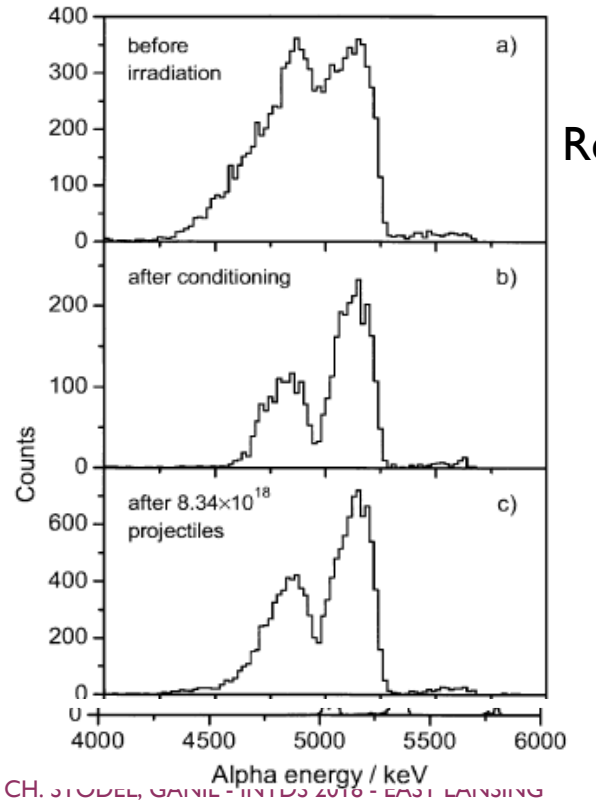

Rest of solvent

homogeneous transparent grass-like layer Highly resistant to beam dose

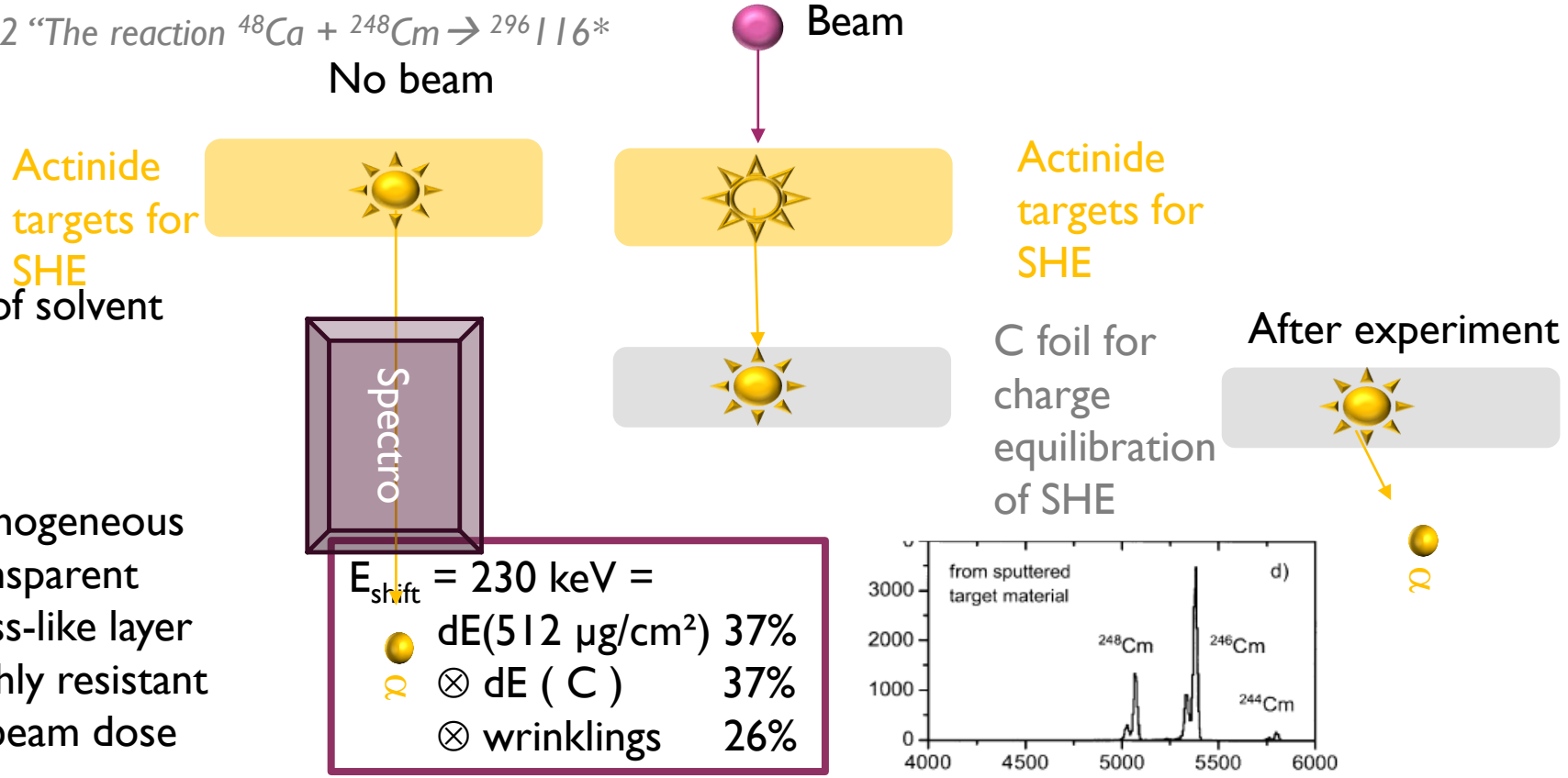

Sputtering of 5-7 µg/10^{18} part /10.7 mg ^{248}Cm

MONITORING OF SHE TARGETS
TUNING ON α EMISSION OF THE TARGETS

2005
^{249}Cf
340 µg/cm²

2015
^{249,250,251}Cf
309 µg/cm²

Evaporation of volatile contaminant

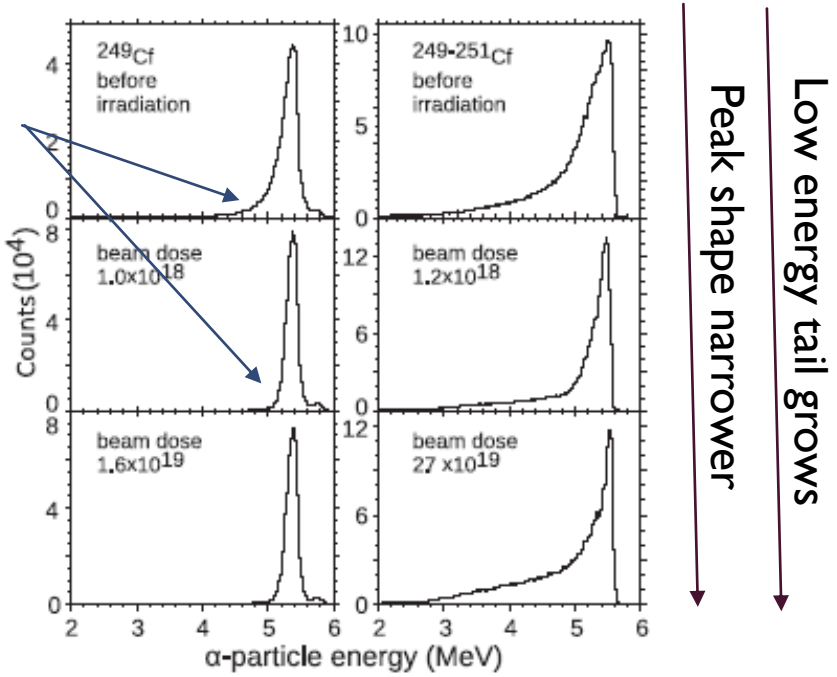

Peak shape narrower

Low energy tail grows

FIG. 6. Spectra of α energies measured from the ^{249}Cf (left panel) and mixed-Cf (right panel) rotating targets with the detector system in the focal plane of DGFRS before irradiations and after given beam doses of ^{48}Ca projectiles passing through the targets.

N. Brewer et al, Phys. Rev. C 98, 024317 (2018) "Search for the heaviest atomic nuclei among products from reactions of mixed-Cf with a ^{48}Ca beam"

Events:
50 pps
.
.
.
.
.
300-350 pps
+ transfer products

→Additional layer == melting &/or evaporation of the gasket and glue

FIG. 7. Target wheel segment before irradiation

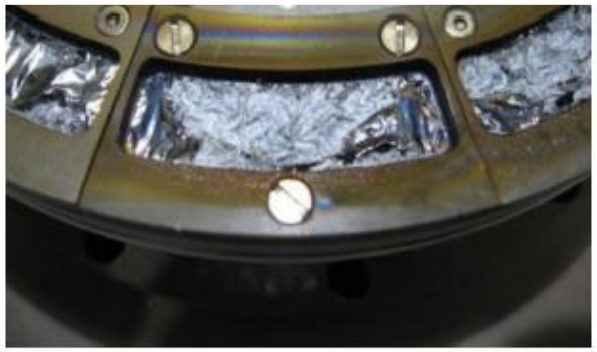

FIG. 8. Target wheel foil after irradiation.

α PARTICLE ENERGY LOSS

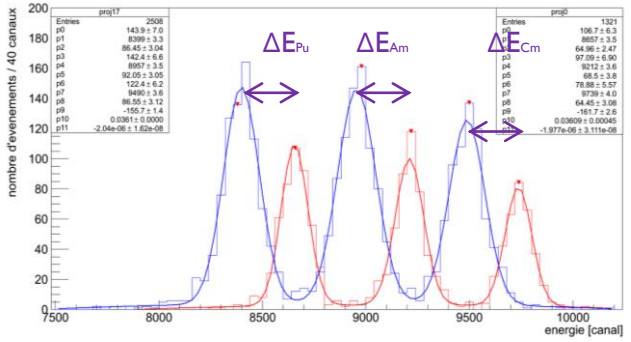

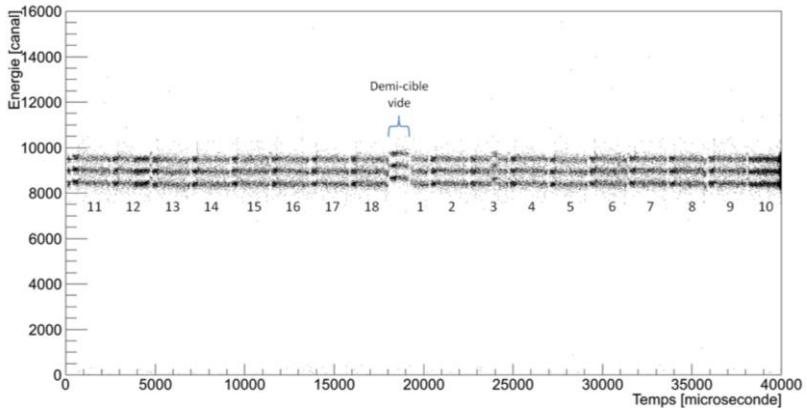

$$x\ [\mu g.cm^{-2}] = \frac{\Delta E\ [keV]}{S(E)\ [(keV.cm^2).\mu g^{-1}]}$$

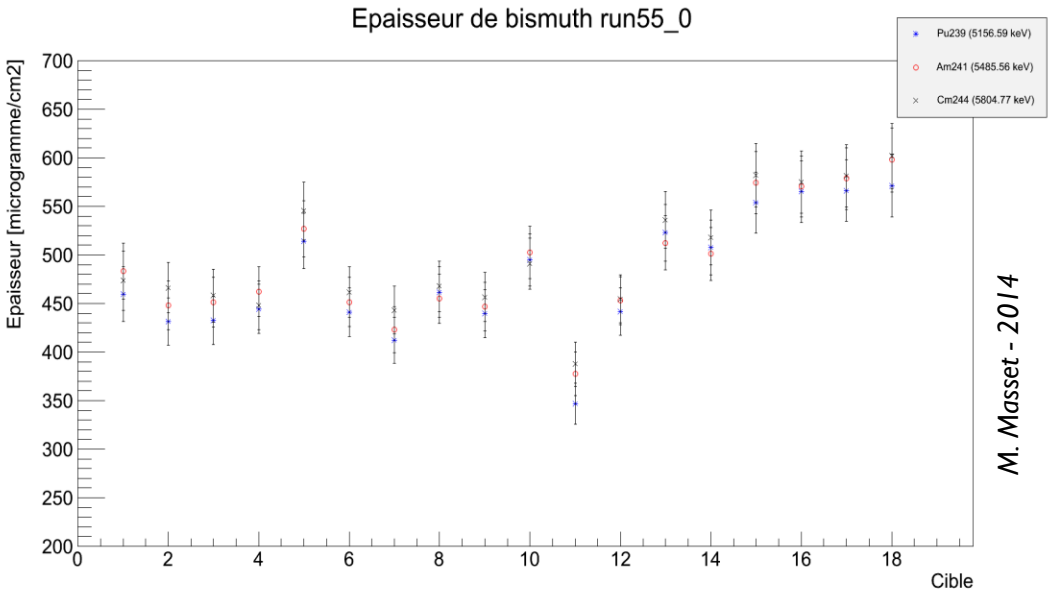

Need of Statistics, e.g. intense α source

SCATTERED PARTICLES WITH HEAVY ION BEAMS

"Rutherford" method

→ Deduced thickness at the beam impact (=f(I, d, θ))

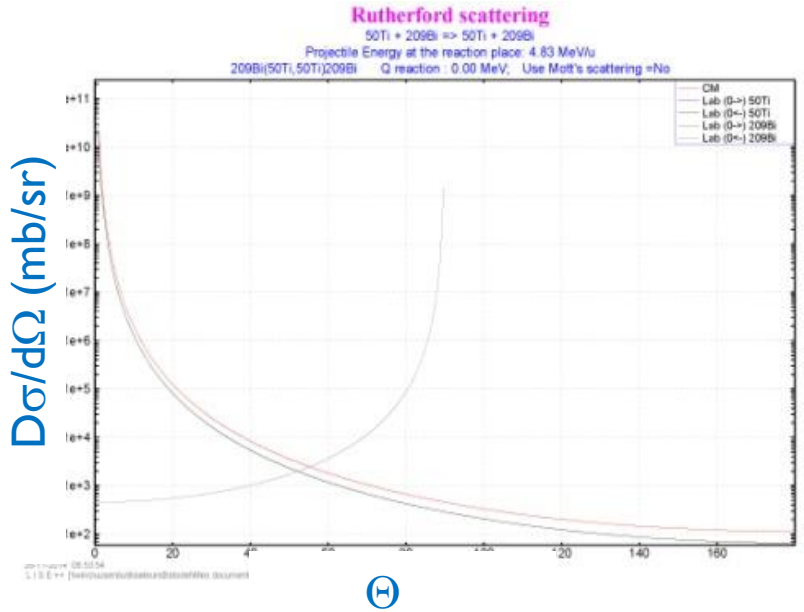

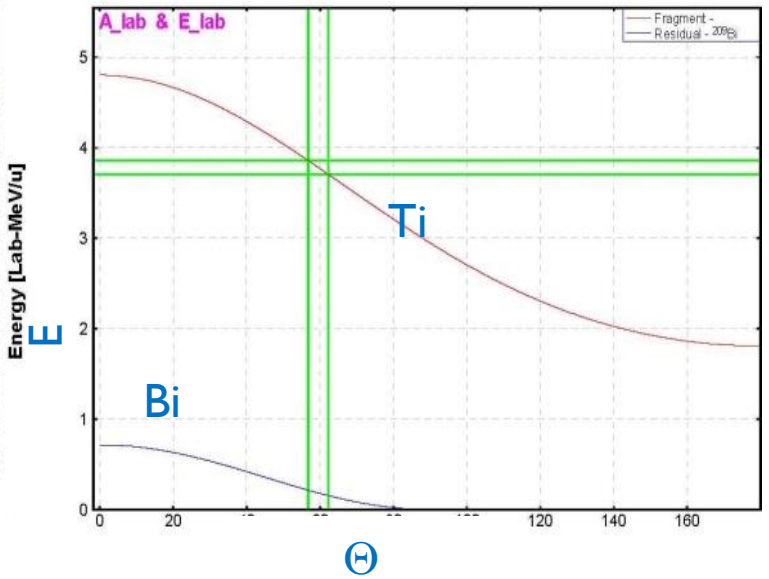

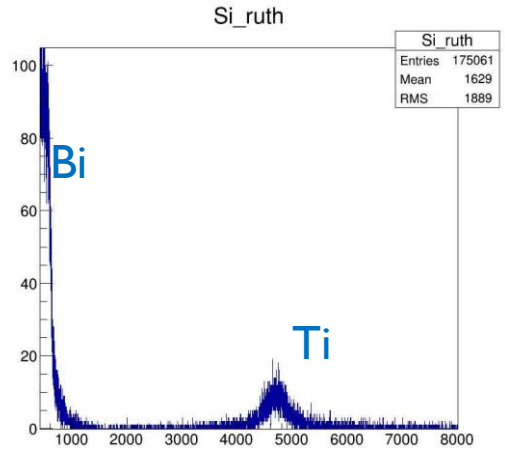

Time to time checking at low intense beam

TEMPERATURE MONITORING

E. Jäger et al, J. Radioanal. Nucl. Chem. (2014) 199:1073-1079 "High Intensity target wheel at TASCA: target wheel control system and target monitoring"

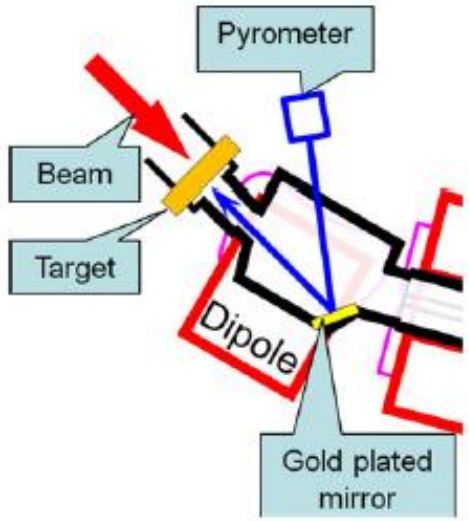

Fig. 5 Position of the pyrometer and light path for monitoring on-line the temperature of the beam-spot of the target

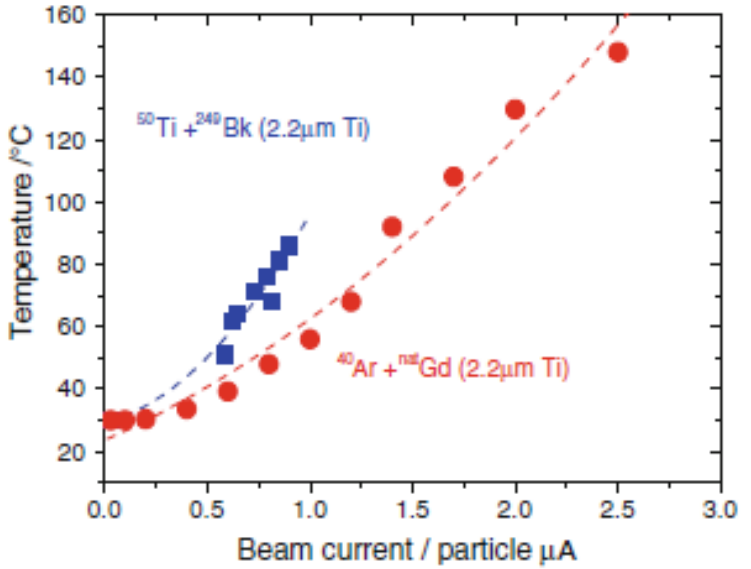

Fig. 6 Target temperature as registered by the pyrometer as a function of the beam intensity. The real maximum temperature may be higher

TEMPERATURE MONITORING: BEAM SPOT PROFILE & TEMPERATURE

A. Yoshida et al, Nucl. Instr. Meth. A590 (2008) 204-212 "Status and overview of production target for BigRIPS separator at RIKEN"

Challenges:

- High-radiation environment → shielding → large distance → efficient lens/mirrors
- Small beam spot
- Precise adjustement of the measuring position ($\overline{T}on$ ☞ $\approx 5\ mm$ & $\Phi(spot) \approx 3mm$) → laser pointer
- Overall emissivity → movable temperature calibrator (Be plate + heater + thermo-couple)

TEMPERATURE MONITORING: BEAM SPOT PROFILE & TEMPERATURE

A.Yoshida et al, Nucl. Instr. Meth.A590 (2008) 204-212 "Status and overview of production target for BigRIPS separator at RIKEN"

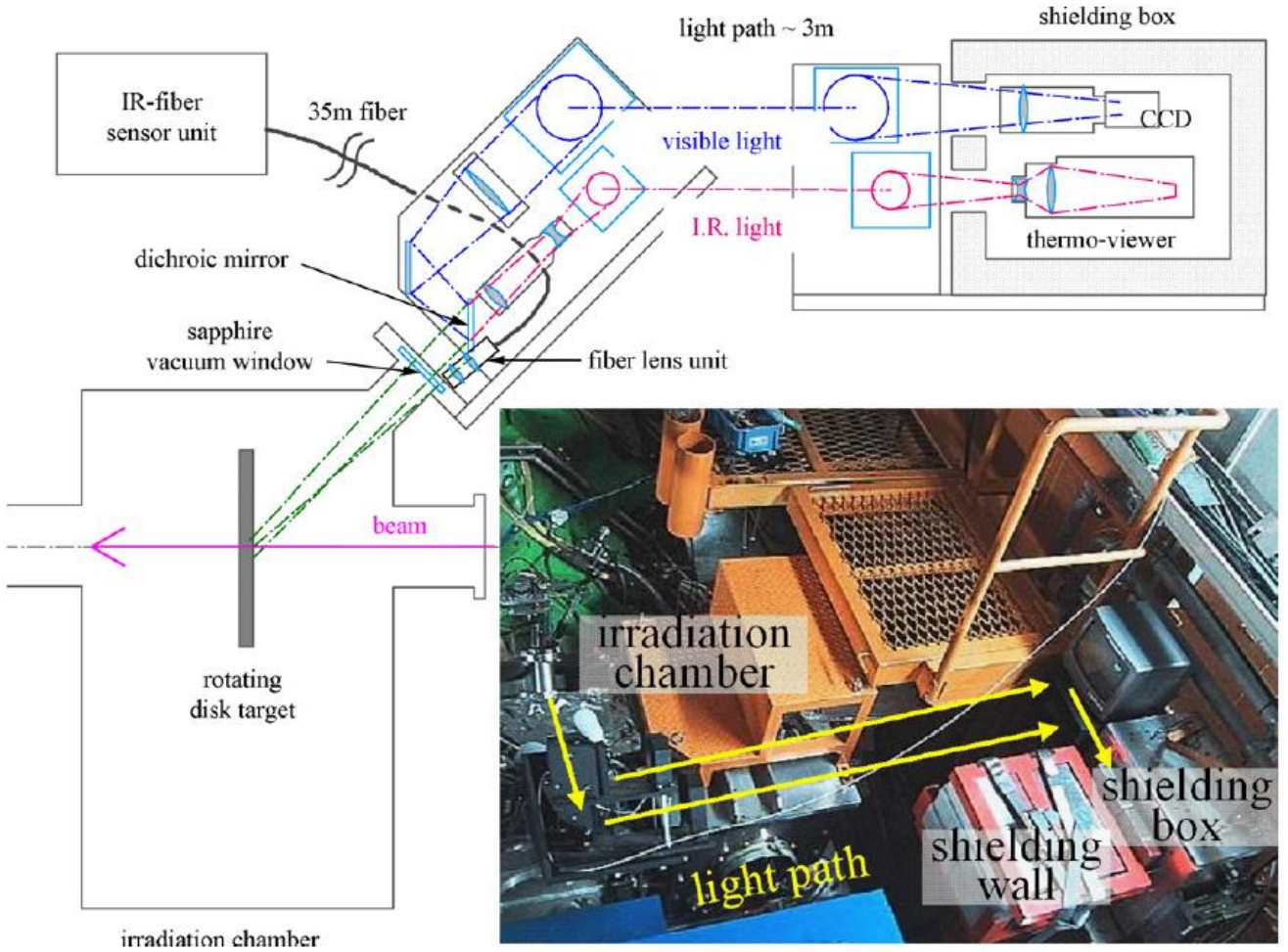

<18 mSv/h

Position resolution achieved = 0,5mm on target

Fig. 3. The beam spot monitoring system for the present RIPS. In a shielding box, a CCD camera and a thermo-viewer are installed. In the light path between the target position and the shielding box, mirror units for visible light and infrared are assembled. The lens unit of the infrared fiberscope is also attached on the sapphire vacuum window.

TEMPERATURE MONITORING: BEAM SPOT PROFILE & TEMPERATURE

A.Yoshida et al, Nucl. Instr. Meth. A655 (2011) 10-16 "Beam-spot temperature monitoring on the production target at the BigRIPS separator"

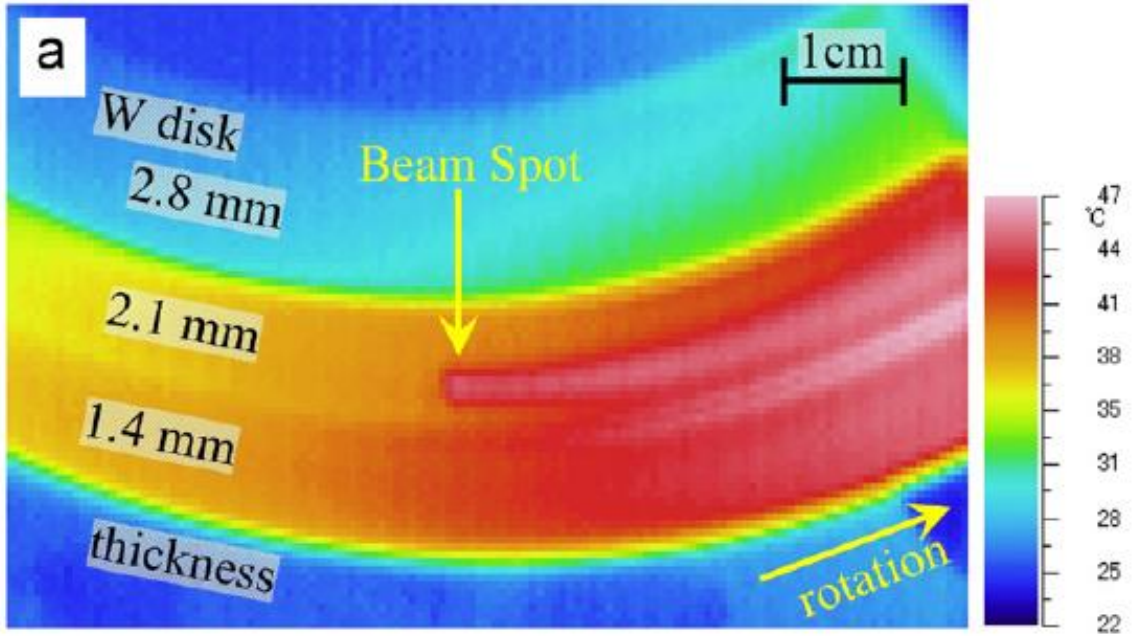

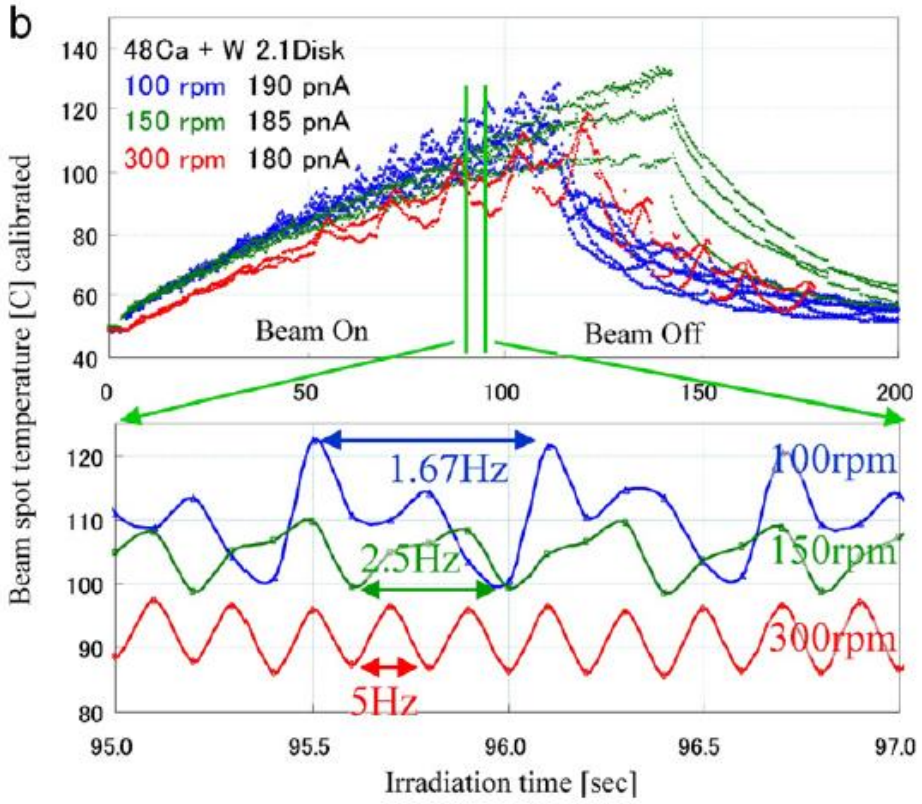

Fig. 9. (a) Observed temperature image of W-disk target rotating with 150 rpm irradiated with a ^{48}Ca-beam of 185 pnA. (b) Beam-spot temperature along with irradiation time for different rotation speeds. Magnified plot (lower graph) shows the periodic temperature vibration observed.

APPLICATION IN PLURIDISCIPLINARY RESEARCH

SCALP
Synthesis & Characterization using ion AcceLerators for Pluridisciplinary research

platform

CSNSM

Synthesis & Characterization using ion Accelerators for Pluridisciplinary research

C.Bachelet, C.-O.Bacri,
C. Baumier, J. Bourçois, L. Delbecq, D.Ledu, N. Pauwels, S. Picard, S. Renouf, C. Tang….

C.O. Bacri et al, Nucl. Instr. Meth. B406 (2017) 48-52

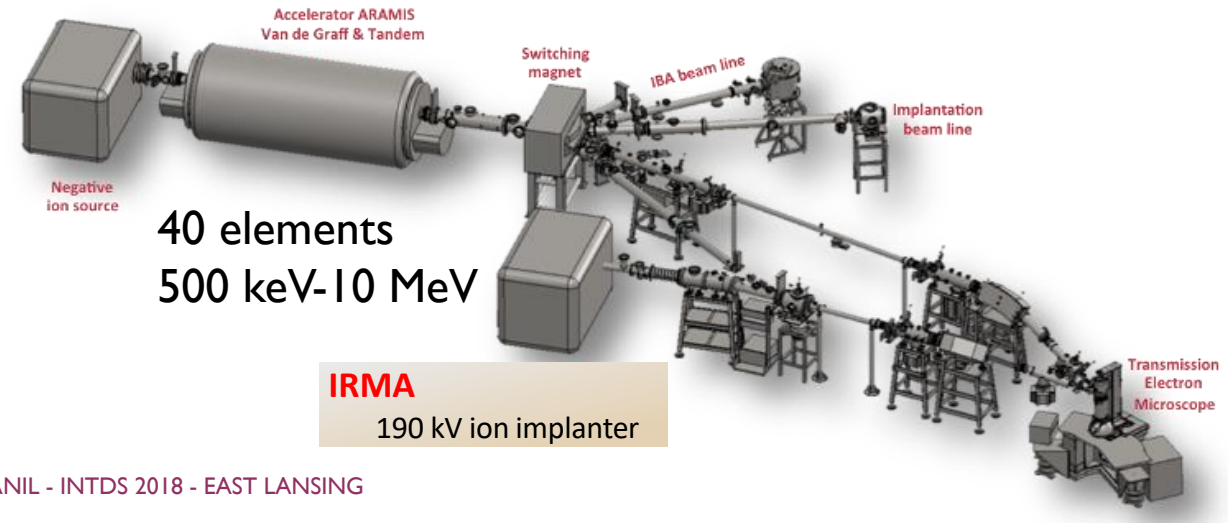

40 elements
500 keV-10 MeV

IRMA
190 kV ion implanter

	High resolution camera 30 frames / sec	
	EDX (Energy Dispersive X-ray spectrometer)	Chemical information down to Be
Energy filter	EELS (Electron Energy Loss Spectroscopy)	Chemical information
	STEM (Scanning Transmission Electron Spectroscopy)	Structural and compositional information sub-nanometer scale
	HAADF (High Angle Annular Dark Field)	Scan images with contrast related to Z

PERFORMANCE / LIFETIME – CARBON CASES

FACTORS

Instant & average temperature rise, mechanical stress & displacement, fatigue due to thermal buckling, sublimation, radiation damage and structure.

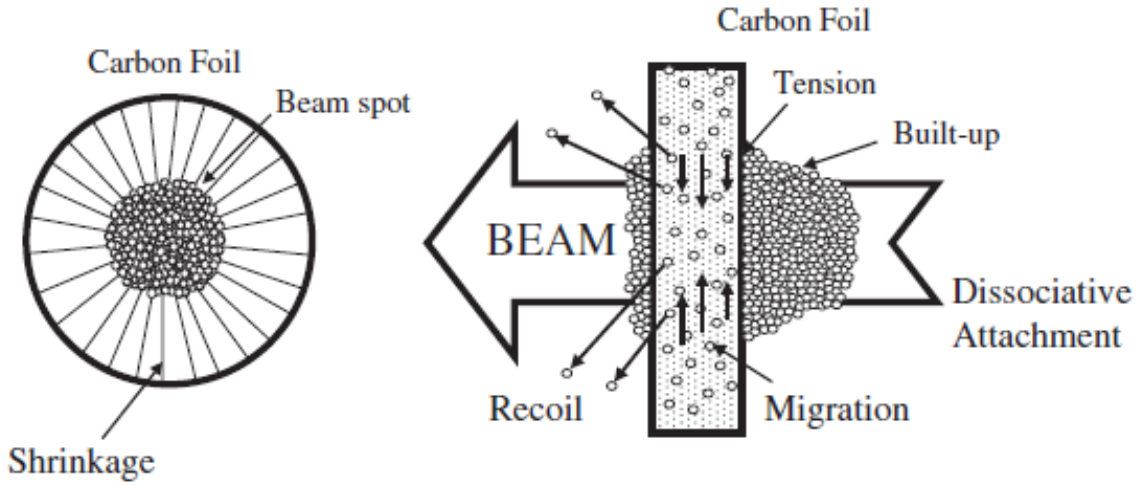

Fig. 1. Schematic illustration of carbon buildup on carbon stripper foil during ion beam irradiation. Buildup can be controlled by a heating method.

I. Sugai et al, Nucl. Instr. Meth. A590 (2008) 32

PERFORMANCE / LIFETIME – CARBON CASES

METHODS

Irradiation with known characteristics: Energy, beam current, beam shape

- Lifetime == ion beam current in mC/cm² until the foil was broken
- Thickness with a SSD at 22,5° downstream

I. Sugai et al, Nucl. Instr. Meth. A590 (2008) 32 & 37

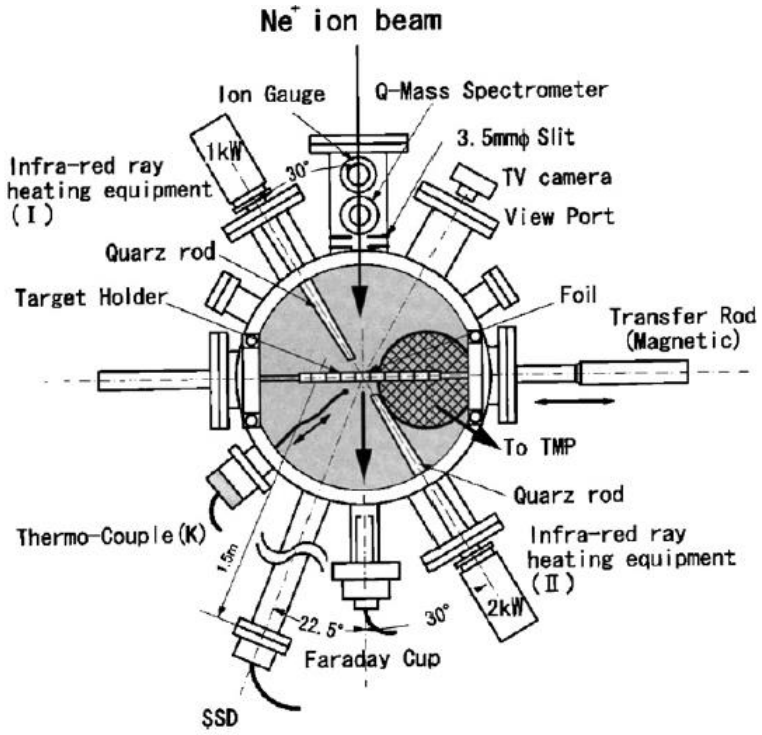

Fig. 4. Experimental setup for controlling and testing the carbon buildup and the lifetime measurements of thin carbon stripper foils. Foils were irradiated using a 3.2Mev Ne^+ ion beam provided from the Van de Graaff accelerator at Tokyo Institute of Technology.

PERFORMANCE / LIFETIME – CARBON CASES

METHODS

Irradiation with known characteristics: Energy, beam current, beam shape

- Monitoring both the beam intensity and C-foil image on a TV display.
- Conditions considering a foil is spent: (a) beam spills along the beamline or on the target collimators reached the warning or trip level & (b) beam spills could not be reduced by returning the available steering & focusing devices.

H. Hasebe et al, Nucl. Instr. Meth. A590 (2008) 13

S.K. Zeisler et al, Nucl. Instr. Meth. A590 (2008) 18

SUMMARY ON THIN LAYERS CHARACTERIZATION & MONITORING

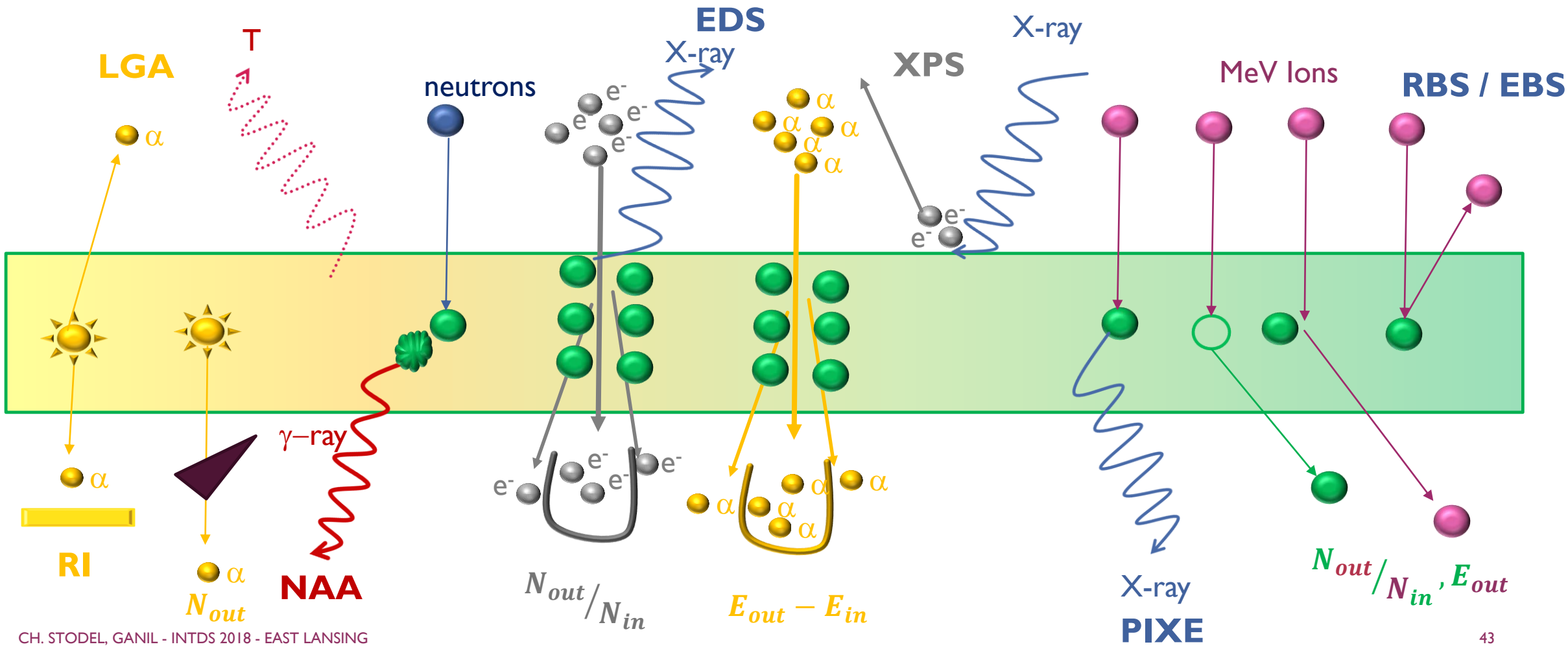

PERSPECTIVE

INTDS encourages the sharing of techniques

The INTDS web page ?

Technique	Laboratory	Description

Masters, School…..

Feel free to use, correct, complete this presentation

Many Thanks to
Klaus, Goedele, Birgit, Bettina

Olivier, François